JNeurosci
THE JOURNAL OF NEUROSCIENCE

Research Articles: Behavioral/Cognitive

Cannabidiol Counteracts the Psychotropic Side-Effects of Δ-9-Tetrahydrocannabinol in the Ventral Hippocampus Through Bi-Directional Control of ERK1-2 Phosphorylation

https://doi.org/10.1523/JNEUROSCI.0708-19.2019

Cite as: J. Neurosci 2019; 10.1523/JNEUROSCI.0708-19.2019

Received: 28 March 2019
Revised: 16 August 2019
Accepted: 3 September 2019

Cannabidiol Counteracts the Psychotropic Side-Effects of Δ-9-Tetrahydrocannabinol in the Ventral Hippocampus Through Bi-Directional Control of ERK1-2 Phosphorylation

Roger Hudson[1,2], Justine Renard[1,2], Christopher Norris[1,2], Walter J. Rushlow[1,2,3] and Steven R. Laviolette[1,2,3]*

[1] Addiction Research Group; [2] Department of Anatomy and Cell Biology; [3] Department of Psychiatry

Schulich School of Medicine & Dentistry

University of Western Ontario, London, Ontario, Canada. N6A 3K7

Running Title: CBD Offsets THC via Hippocampal ERK1-2 Signaling

Number of Pages: 54

Number of Figures: 6; Tables: 0.

Number of Words: Abstract: 153 words; Introduction: 624 words; Discussion: 2,166 words

Acknowledgments: This work was supported by the Canadian Institutes of Health Research (CIHR), the National Science and Engineering Research Council of Canada (NSERC), MITACs and a Vanier CGS awarded to RH.

Conflict of Interest: The authors have no conflict of interest to disclose.

***Corresponding Author**

Steven R. Laviolette, Ph.D.

Department of Anatomy and Cell Biology

University of Western Ontario

London, Ontario, Canada, N6A 3K7

e-mail: steven.laviolette@schulich.uwo.ca

Abstract

Evidence suggests that the phytocannabinoids Δ-9-tetrahydrocannabinol (THC) and cannabidiol (CBD) differentially regulate salience attribution and psychiatric risk. The ventral hippocampus (vHipp) relays emotional salience via control of dopamine (DA) neuronal activity states, which are dysregulated in psychosis and schizophrenia. Using *in-vivo* electrophysiology in male Sprague Dawley rats, we demonstrate that intra-vHipp THC strongly increases ventral tegmental area (VTA) DA neuronal frequency and bursting rates, decreases GABA frequency, and amplifies VTA beta, gamma and epsilon oscillatory magnitudes via modulation of local extracellular signal-regulated kinase phosphorylation (pERK1-2). Remarkably, whereas intra-vHipp THC also potentiates salience attribution in morphine place-preference and fear conditioning assays, CBD co-administration reverses these changes by down-regulating pERK1-2 signaling, as pharmacological re-activation of pERK1-2 blocked the inhibitory properties of CBD. These results identify vHipp pERK1-2 signaling as a critical neural nexus point mediating THC-induced affective disturbances and suggest a potential mechanism by which CBD may counteract the psychotomimetic and psychotropic side-effects of THC.

Significance Statement

Strains of marijuana with high levels of delta-9-tetrahydrocannabinol (THC) and low levels of cannabidiol (CBD) have been shown to underlie neuropsychiatric risks associated with high potency cannabis use. However, the mechanisms by which CBD mitigates the side effects of THC have not been identified. We demonstrate that THC induces cognitive and affective abnormalities resembling neuropsychiatric symptoms directly in the hippocampus, while dysregulating dopamine activity states and amplifying oscillatory frequencies in the ventral tegmental area via modulation of the extracellular signal-regulated kinase (ERK) signaling pathway. In contrast, CBD co-administration blocked THC-induced ERK phosphorylation, and prevented THC-induced behavioural and neural abnormalities. These findings identify a novel molecular mechanism that may account for how CBD functionally mitigates the neuropsychiatric side-effects of THC.

Introduction

Chronic or acute use of high-potency cannabis is associated with numerous neuropsychiatric side-effects, including dysregulation of emotional processing and associative memory formation (Di Forti et al., 2009). However, given the phytochemical complexity of cannabis, increasing evidence suggests highly divergent psychotropic effects following exposure to distinct cannabis constituents. Thus, while the neuropsychiatric side-effects of cannabis are associated with Δ-9-tetrahydrocannabinol (THC), clinical and preclinical findings demonstrate that cannabidiol (CBD), the major non-psychoactive phytocannabinoid in cannabis, possesses antipsychotic and anxiolytic properties (Leweke et al., 2012; Zuardi et al., 2006). Indeed, whereas THC induces dysregulation of subcortical dopamine (DA) transmission and affective salience processing (Bhattacharyya et al., 2012; Palaniyappan et al., 2013; Renard et al., 2017), CBD normalizes aberrant DA signaling and regulates affective stimulus processing (Norris et al., 2016; Renard et al., 2016a). Nevertheless, the precise neurobiological mechanisms by which CBD may mitigate the neuropsychiatric side-effects of THC are not understood.

The ventral hippocampus (vHipp) is an integrative structure sub-serving mesocorticolimbic DA signaling and emotional processing and is implicated in schizophrenia-related neuropathology (Grace, 2010). For example, disinhibition of the vHipp distorts emotional salience and induces a schizophrenia-like phenotype by dysregulating activity of ventral tegmental area (VTA) DA neurons and mesolimbic DA transmission (Floresco et al., 2001; Legault et al., 2000; Loureiro et al., 2015). vHipp morphometric abnormalities and dysregulated connectivity between the vHipp and frontotemporal structures are pathological features of schizophrenia (Meyer-Lindenberg et al., 2005; Szeszko et al., 2003). Importantly,

use of THC-rich cannabis induces vHipp abnormalities and learning and memory disturbances that are mitigated by CBD (Beale et al., 2018; Bhattacharyya et al., 2010; 2015; Englund et al., 2013). Thus, pathological vHipp overdrive may represent a convergent link contributing to disturbances in affective salience processing and memory function observed in schizophrenia and following THC exposure (Laviolette and Grace, 2006).

CBD mitigates psychosis-like neuronal, behavioural and molecular endophenotypes associated with schizophrenia, for example, by inhibiting amphetamine and MK-801-induced dysregulation of DA transmission, and associated beta (β) and gamma (γ) oscillatory patterns in reverse-translational schizophrenia models (Benes et al., 2006; Gomes et al., 2015; Moreira and Guimarães, 2005; Renard et al., 2016a; b). Furthermore, CBD counteracts several signal transduction cascades associated with THC-induced impairments, including the hippocampal mitogen-activated protein kinase/extracellular signal-regulated protein kinase (ERK) pathway (Derkinderen et al., 2003; Elbaz et al., 2015; Solinas et al., 2013). Considering that vHipp dysfunction is common to THC-induced neuropsychiatric impairments and schizophrenia, one possibility is that the antipsychotic properties of CBD are attributable to competing actions by CBD on local vHipp function.

In the present study, we investigated the hypothesis that intra-vHipp THC and CBD differentially impact emotional memory processing and VTA neural activity via distinct actions within the vHipp ERK signaling pathway. To elucidate the specificity of THC on the vHipp ERK signal transduction cascade, we co-administered THC alongside the highly selective and potent MEK1-2 inhibitor, U0126, which functionally antagonizes AP-1 transcription via MEK inhibition (Duncia et al., 1998). Additionally, to characterize the properties of combined THC+CBD on ERK activity, we co-administered THC+CBD alongside eicosapentaenoic acid

(EPA), which promotes ERK phosphorylation via interaction with Thr235 and increases in upstream rate-limiting H-Ras protein expression levels. We report that intra-vHipp THC potentiates the affective salience of normally non-salient rewarding and aversive memory cues, while increasing VTA DA neuronal activity states, decreasing VTA GABAergic activity, and concomitantly amplifying β, γ, and epsilon (ε) oscillatory frequencies within the VTA via an ERK-dependent mechanism. Remarkably, CBD co-administration reversed THC-induced changes in VTA neural activity and emotional memory processing via down-regulation of vHipp ERK phosphorylation states. These findings identify for the first time a precise molecular and neuronal mechanism by which CBD may mitigate the neuropsychiatric side-effects of THC directly in the vHipp, a brain region known to be pathologically impacted by cannabis exposure and schizophrenia.

Materials and Methods

Subjects

Male Sprague-Dawley rats (Charles River, St-Constant, Quebec) weighing 250-300 g at the start of experiments were single-housed under controlled conditions (22–23° C, lights on at 07:00, lights off at 19:00) with ad-libitum access to food and water. All experimental protocols were approved by the Animal Care and Veterinary Services Committee at Western University and were carried out in accordance with recommendations provided by the Canadian Council on Animal Care.

Surgical Procedures

Rats were anesthetized with a 2:1 mixture of ketamine (100 mg/ml; Narketan, Belleville, Canada) and xylazine (20 mg/ml; Bayer, Mississauga, Canada) and placed in a stereotaxic device. Stainless steel guide cannulae (22 gauge, Plastics One) were implanted bilaterally into the vHipp at the following coordinates: AP: -5.6 mm from bregma, LM: ±5.0 mm, DV: -6.8 mm from the dural surface. Guide cannulae were secured in place using jeweler's screws and dental acrylic cement. To minimize pain and inflammation, meloxicam (1 mg/kg, s.c.; Boehringer Ingelheim, Burlington, Canada) was administered before surgeries and on the initial post-operative day. Behavioral testing began one-week post-recovery. Following completion of behavioral experiments, rats received an overdose of sodium pentobarbital (240 mg/kg, i.p., Euthanyl) and brains were extracted and post-fixed 24 hours in 10% formalin before being placed in a 25% formalin-sucrose solution for 1 week. Brains were sliced (60 µm) using a cryostat and stained with Cresyl violet. Injector tip placements were localized using a light microscope. Rats with cannula placements found outside the anatomical boundaries of the vHipp (as defined by Paxinos and Watson, 2007) were excluded from data analysis (n=7 total). An additional eight rats were removed from subsequent experiments following blockade of cannulae throughout the series of experiments.

Drug administration

The following drugs were used during behavioral or electrophysiological experiments: THC (Cayman Chemical, Ann Arbor, Michigan, USA), CBD (Tocris Bioscience, Bristol, United Kingdom), the selective MEK1/MEK2 inhibitor U0126 (Tocris), the omega-3 fatty acid eicosapentaenoic acid (EPA; Tocris), sucrose (Sigma-Aldrich) and

morphine sulphate (Johnson-Matthey). THC, and EPA in ethanol were each dissolved in cremophor and saline (1:1:18). Nitrogen gas was used to evaporate ethanol from the final THC and EPA solutions. CBD was dissolved in cremophor and saline (1:18). U0126 was dissolved in DMSO and then diluted in sterile saline to achieve a 25% DMSO concentration. Morphine sulphate was dissolved in physiological saline, with pH adjusted to 7.4. A solution of cremophor and saline (1:18) was infused as a Vehicle control.

Intra-vHipp microinfusions were performed immediately before each behavioural assay or conditioning session. A total volume of 0.5 mL per hemisphere was delivered via 28-gauge microinfusion injectors over 1 min. To ensure adequate drug diffusion, microinjectors were left in place for an additional one-minute following drug infusion.

Protein Expression Analyses

To evaluate the local effects of intra-vHipp phytocannabinoids on expression of pERK, ERK, and the ratio of pERK:ERK, a subset of rats received bilateral intra-vHipp microinfusions of vehicle (VEH), THC (100 ng), CBD (100 ng), THC+CBD (100 ng + 100 ng), THC+U0126 (100 ng + 1 μg) or THC+CBD+EPA (100 ng + 100 ng + 1 mM) five minutes prior to being euthanized. Brains were rapidly removed, and flash frozen at -80°C. Coronal sections (95 μm) containing the vHipp were cut on a cryostat and slide mounted. Bilateral microdissections surrounding the injector sites were obtained (~2.5 mg total tissue per subject), using light microscopy to identify and avoid any regions with reactive gliosis. The western blotting procedure was performed as described previously (Lyons et al., 2013) using approximately 12.5 μg of collected tissue per blot. Primary antibody dilutions were as follows: α-tubulin (1:1,000,000; Sigma-Aldrich), pERK (1: 1,000, Cell

Signaling Technology (CST), and ERK (1: 2,000, CST). Species appropriate horseradish peroxidase (HRP)-conjugated secondary antibodies (LI-COR IRDye 680RD and IRDye 800CW, Thermo Scientific) were each used at a dilution of 1: 10,000. Densitometry measurements were obtained using Li-Cor Odyssey digital imaging software and Image Studio analysis software by normalizing the intensity of each sample's target protein band to the respective α-tubulin intensity.

VTA Neuronal Activity Recordings and Analysis

Extracellular single-unit electrophysiological recordings were performed in-vivo in adult rats weighing 300-450 g. The recordings were taken either from putative dopaminergic (DA) VTA neurons or from non-DA GABAergic VTA neurons. In-vivo extracellular single-unit recordings in the VTA were performed as described previously (Loureiro et al., 2015). Briefly, rats were anesthetized with urethane (1.5 g/kg, i.p., Sigma-Aldrich) and placed in a stereotaxic frame with body temperature maintained at 37 °C. A scalp incision was made, and holes were drilled in the skull overlaying the VTA and vHipp. For intra-vHipp microinfusions, a 10 μL Hamilton syringe was slowly lowered into the vHipp using the stereotaxic coordinates described above. For intra-VTA recordings, glass microelectrodes (average impedance of 6–8 MΩ) filled with a 2 M sodium acetate solution containing 2% pontamine sky blue were lowered with a hydraulic micro-positioner (Kopf640) to the following coordinates: AP: -5.0 mm from bregma, L: ±0.7 mm, DV: -7.0 to -9.0 mm from the dural surface. A bone screw was placed over the cerebellum and connected with the return of the headstage, serving as a reference electrode. The electrophysiological properties of spontaneously active neurons were sampled by vertically passing the electrode through the

VTA cell body region. A minimum washout duration of 1-hour was allowed between intra-vHipp infusions. Vertical tracks were made in a predefined pattern, with each track separated by 200 μm.

Extracellular signals were amplified (x5000) using a MultiClamp700B amplifier (Molecular Devices), digitized at 25 kHz and recorded through a Digidata1440A acquisition system (Molecular Devices) and pClamp10 software. Wideband VTA signal recordings were fed through two channels of the digitizer and filtered to obtain single unit recordings (band pass between 0.3 and 3 kHz) and local field potentials (LFPs; low pass at 0.3 kHz). VTA DA neurons were identified according to well established electrophysiological features (Grace and Bunney, 1983): (1) a relatively long action potential width (>2.5 ms), (2) a slow, spontaneous firing rate (2–9Hz), (3) a triphasic waveform consisting of a notch on the rising phase followed by a delayed after potential, and (4) a single irregular or bursting firing pattern. In contrast, VTA non-DAergic cells were characterized based upon: (1) a narrow action potential width (<1 ms), (2) a biphasic waveform, (3) relatively fast firing rates (>10 Hz), and (4) the absence of burst firing.

Electrophysiological analyses were performed using the Clampfit10 (Molecular Devices) software package. Firing frequencies of isolated VTA neurons following intra-vHipp microinfusions were normalized to the respective baseline firing frequency. The response patterns of VTA neurons to vHipp microinfusions were determined by comparing the neuronal frequency rates between the 5-minute preinfusion versus postinfusion recording epochs. The 5-minute preinfusion epoch was commenced following at least 2 minutes of stable physiological (single unit and LFP) activity. The 5-minute postinfusion epoch commenced immediately following the 1-minute intra-vHipp infusion. We ensured minimum

1-hour delay between recordings to prevent effects infusions, and recordings within each animal were carried out within 1 drug condition. Classification of drug infusion effects used a criterion of >10% change in firing frequency relative to pre-infusion to be classified as an 'increase' or 'decrease' effect. Neurons displaying <10% change in firing frequency parameters after infusion were classified as 'no change'. In VTA DA neurons, we also analyzed the proportion of action potentials firing in the phasic bursting modality. The onset of a burst event was defined as the occurrence of two or more consecutive spikes within an interspike interval of <80 ms.

LFP signals were analyzed using NeuroExplorer (Nex Technologies). Recordings were first decimated to 1 kHz, and lowpass filtered (IIR Butterworth filter at 170 Hz; filter order set to 3). A spectrogram function was then used to calculate the power of oscillations at frequencies between 0–100 Hz (window length 2 s; shift 0.5 s). Pre-infusion and post-infusion parameters remained the same as outlined previously. Power values for a given frequency were averaged over the recording epoch and normalized so that the sum of all power spectrum values equals 1. The total power was calculated by adding the power values at frequencies between 0–59 and 61–100 Hz, and power values at 60 ± 1 Hz were excluded from all calculations. Neural oscillations were defined within specific frequency bands as follows: delta band, 0-4 Hz; theta band, 4-7 Hz; alpha band, 7-14 Hz; β band, 14-30 Hz; γ band, 30–80 Hz; and ε band, 90-100 Hz. Every recording was taken at a different electrode location throughout VTA.

Positions of recording electrodes were marked with an iontophoretic deposit of pontamine sky blue dye (-19.5 mA, continuous current for 15 min) for histological analyses, which were performed as described previously (Renard et al., 2017). Recordings obtained

from two rats were excluded from electrophysiological data analysis because histological analysis revealed iontophoretic deposits beyond the anatomical boundaries of the VTA as defined by Paxinos and Watson (2007).

Behavioural Testing

A battery of behavioural assays was conducted to examine the effects of acute intra-vHipp THC vs CBD infusions on affective and anxiety-related behaviours. Between experiments, rats were returned to the home cage for a minimum of 3 days. Rats were randomly assigned across experiments and counterbalanced within groups. Separate cohorts of rats received the conditioned place preference, context-dependent, or context-independent fear conditioning procedures as final tests, as these (opiate exposure and high stress) tests were considered terminal. We performed the following ordered series of behavioural assays:

Open field test

Rats were placed in an automated open field activity chamber (Med Associates, Fairfax, VT) for 30 min. Total distance moved, time spent inactive in the centre compartment of the chamber (initial 5 mins only), and stereotypy times were recorded and analyzed. Time spent inactive in the centre compartment relative to the outer compartment were measured as an index of anxiety as higher states of anxiety are associated with lower exploration times in the central regions of the open field chamber and greater times spent in the peripheral zone (Ohl et al., 2003). Stereotypy was defined as time spent mobile within a software-generated, pre-defined zone in the open field chamber. At time zero, the program centres this pre-defined zone on the subject. When the subject moves outside this zone, the activity

is considered ambulatory and the zone re-centres on the subject. If the subject remains inside the re-centred zone for longer than a software-defined resting delay (2,500 ms), the subject's activity is considered stereotypic until they move outside the zone.

Light dark box

This test exploits a rat's natural aversion to bright environments and attributes greater time spent in an illuminated environment as reflecting lower anxiety levels. The test was performed as previously described (Renard et al., 2016a). At the start of the experiment, a rat was placed in the center of the lighted box with its head facing the wall opposite the door and allowed to freely explore both compartments for 8 min. A zone entry was considered to have begun when the rat placed all 4 paws in that zone. Experiments were videotaped with an automated video-tracking system (ANY-maze; Stoelting, Wood Dale, IL). Behaviors analyzed included % time in light side, and latency to second transition (latency time to exit the dark box and re-enter the light box), which are each robust indicators of anxiety-like behavior and sensitive to both anxiogenic and anxiolytic treatments[62].

Sucrose preference test

To allow for acclimation to a palatable liquid-sucrose solution, rats received 48 hours ad-libitum access to 2% sucrose solution in bottles suspended in their home cages, without access to water. Following acclimation, rats were deprived of water and 2% sucrose solution for 12 hours before testing. During the 1-hour test, rats were given ad-libitum access to two bottles – one containing water and one containing 2% sucrose solution. Fluid volumes

consumed during testing were normalized according to body weight and sucrose preference was calculated and expressed as % of total fluid intake.

Context-dependent and context-independent fear conditioning

To study the effects of intra-vHipp phytocannabinoids on aversive memory processing, rats were tested in context-dependent or context-independent olfactory cue fear conditioning procedures as described previously (Loureiro et al., 2016). During context-dependent fear conditioning, associative contextual stimuli of the context (black and white stripes, or polka dots) were paired through counterbalancing with subthreshold levels of footshock (10 shocks, 1 second, .4 mA, administered at random time intervals during a single 20 minute conditioning session) that we have previously shown do not produce significant fear memories (Loureiro et al., 2016). 24 hours following conditioning, subjects were re-exposed for 10 minutes to the conditioning context for testing, in a drug-free state. For the context-independent fear conditioning protocol, subjects were habituated for 30 minutes to the 'safe' context 24 hours prior to conditioning. Two odors were used during context-independent olfactory fear conditioning in the 'shock' context – almond and peppermint fragrance oils. One odor was paired with a footshock (conditioned stimulus [CS]+), and the other paired with the absence of footshock (CS-) in a counterbalanced fashion. 10 CS+ and 10 CS- pairings were presented during the 20-minute conditioning session. 24 hours following conditioning, subjects were re-exposed for 5 minutes to each CS in a counterbalanced style for testing, in a drug-free state. Time freezing was recorded over 10 minutes using automated video tracking (ANY-maze).

Conditioned place preference

We employed a conditioned place preference (CPP) procedure, as previously described (Lintas et al., 2011). Briefly, subjects were habituated to a neutral grey context for 20 minutes the day before conditioning onset. For conditioning days, saline or morphine injections (i.p.) were paired with one of two environments that differed in color (black vs white), texture (plexiglass floor vs bedding), and smell (0.4 mL of 2% acetic acid vs woodchips scent). For CPP testing, rats are given the free choice to spend time in either of the previously experienced (Drug vs. Veh) conditioning environments, which are separated by a narrow (10 cm) grey strip of Plexiglas. As reported previously, rats display no baseline preference for either of these two environments (Laviolette and van der Kooy, 2003). Rats received four morphine-environment and four saline-environment conditioning sessions (1 session per day on alternating days, 8 days conditioning in total) in a fully counterbalanced design. We used a sub-reward threshold conditioning dose of morphine (0.05 mg/kg i.p.) that we have previously demonstrated to produce no significant CPP (Lintas et al., 2011). Rats received i.p. injections immediately before being placed in saline- or morphine-paired environments for conditioning sessions lasting 30 minutes each. Intracranial microinfusions directly preceded i.p. injections and were given before all conditioning trials. Two days following conditioning, rats were tested (drug-free) for place preference during a 10-minute test, and times spent in each environment were recorded with an automated video-tracking system (ANY-maze). CPP behavior is expressed as % time spent in morphine and saline-paired environments.

Statistical Analyses

The data were analyzed using one or two-way analyses of variance (ANOVA) followed by Newman Keul's (electrophysiological data) or Fisher's LSD tests (molecular and behavioural analyses) for multiple comparisons (alpha < 0.05). When appropriate, planned comparisons were performed using t-tests, as indicated. All analyses were performed using Sigmaplot (version 12.0 for Windows), and only the exact values of significant analyses are reported.

Results

THC and CBD differentially regulate local ERK1-2 phosphorylation states in the vHipp

At the molecular level, THC and CBD differentially modulate cellular ERK1-2 signaling, with THC activating and CBD inhibiting ERK1-2 phosphorylation (Derkinderen et al., 2003; Elbaz et al., 2015). Accordingly, we first examined whether intra-vHipp vehicle (VEH; n=6), THC (100 ng/0.5 μl; n=6), CBD (100 ng/0.5 μl; n=6), or a combination of THC (100 ng) + CBD (100 ng/0.5 μl; n=6) may differentially modulate local vHipp ERK1-2 phosphorylation (pERK1-2) states. To characterize the ability of THC to increase pERK1-2 expression directly in the vHipp we co-administered THC alongside the MEK1-2 inhibitor, U0126 (1 μg; n=5), at a dose previously characterized as having pharmacologically specific actions on neuronal ERK1-2 expression levels (Lyons et al., 2013). In addition, to characterize the actions of THC+CBD on pERK1-2 expression levels, we co-administered the THC+CBD with the ERK-activating agent eicosapentaenoic acid (EPA; 1mM; n=5), at a dose previously described to elevate pERK1-2 phosphorylation (Maher et al., 2004; Salvati et al., 2008).

Mixed measures ANOVA revealed a significant main effect of Group [$F_{(5, 28)}$ = 10.18, $p < 0.001$], but no significant effect of Isoform Factor [$F_{(1, 28)} = 0.328$, $p > 0.05$], or interaction between Group and Isoform Factors [$F_{(5, 28)} = 0.297$, $p > 0.05$]. Post-hoc comparisons using Fisher's LSD on marginal means revealed that THC significantly increased levels of vHipp pERK1-2 expression relative to VEH ($p = 0.001$), CBD ($p < 0.001$), THC+CBD ($p < 0.001$), and THC+U0126 groups ($p = 0.04$). Thus, intra-vHipp THC strongly increases local pERK1-2 expression via upstream MEK1-2 signaling. In contrast, whereas CBD has no significant effects relative to VEH, the THC+CBD combination blocks the effects of THC and significantly downregulates pERK1-2 expression relative to VEH ($p = 0.004$). Furthermore, the THC+CBD decrease of vHipp pERK1-2 activation is reversed by simultaneous pharmacological activation of ERK1-2 ($p < 0.001$; **Figure 1a**).

Figure 1b represents mean % total ERK1-2 expression. Mixed measures ANOVA revealed no significant main effects of Group [$F_{(5, 28)} = 1.05$, $p > 0.05$), Isoform Factor [$F_{(1, 28)} = 0.004$, $p > 0.05$), or interaction between Group and Isoform Factors [$F_{(5, 28)} = 0.584$, $p > 0.05$), indicating that acute intra-vHipp THC, CBD, or THC+CBD infusion did not alter ERK1-2 expression. The pERK:ERK1-2 expression ratio (transformed from raw pERK and tERK data) is represented in **Figure 1c**. Mixed measures ANOVA revealed a significant main effect of Group [$F_{(5, 28)} = 6.88$, $p < 0.001$], but no significant effect of I Isoform Factor [$F(1, 28) = 0.127$, $p > 0.05$), or interaction between Group and Isoform Factors [$F(5, 28) = 0.334$, $p > 0.05$). Post-hoc comparisons using Fisher's LSD revealed that THC significantly increased pERK:ERK1-2 expression ratio relative to VEH ($p = 0.014$), CBD, and THC+CBD groups (p's < 0.001). Thus, whereas intra-vHipp THC strongly increases the pERK:ERK1-2 expression ratio relative to VEH, CBD shows no effects. In contrast, the

389 THC+CBD combination significantly downregulates pERK:ERK1-2 expression, an effect
390 that is reversed via co-administration of THC+CBD+EPA ($p < 0.001$). Representative
391 western blots for pERK1-2 and ERK1-2 expression levels in the vHipp are shown in **Figure**
392 **1d**. In **Figure 1e**, we present a schematic summary of intra-vHipp microinfusion locations for
393 the above described experimental groups.
394
395 ***Intra-vHipp THC and CBD differentially modulate anxiety-like behaviours via local***
396 ***ERK1-2 modulation***
397 We next examined the potential effects of intra-vHipp THC or CBD on a battery of
398 anxiety-related behavioural assays and the potential role of localized ERK1-2 signaling in
399 these effects. First, using the open field test (see methods), we compared total ambulatory
400 activity following THC/CBD administration and anxiety-related spatial exploration
401 parameters. Comparing mean total distance travelled following intra-vHipp microinfusion of
402 VEH (n=11), 10 (n=10) or 100 ng THC (n=12), 10 (n=9) or 100 ng CBD (n=9), or 100 ng
403 THC+CBD (n=8) co-administration, one-way ANOVA revealed no significant main effect of
404 Group [$F_{(5, 53)} = 0.412$, $p > 0.05$], demonstrating that THC/CBD has no effects on gross
405 motoric behaviours (**Figure 2a)**.
406 Next, comparing times spent in the center vs. peripheral zones of the test arena
407 during the initial 5 mins of testing revealed differential effects of THC vs. CBD on anxiety-like
408 behaviours (**Figure 2b**). First, one-way ANOVA comparing times spent in the centre zone
409 between VEH, THC (10 and 100 ng), CBD (10 and 100 ng), and THC+CBD (100 ng)
410 revealed a significant main effect of Group [$F_{(5, 53)} = 4.81$, $p = 0.001$]. Post-hoc comparisons
411 using Fisher's LSD demonstrate that the higher dose of THC (100 ng) decreases time spent

in the centre zone relative to VEH ($p = 0.046$), suggesting a dose-dependent anxiogenic effect. In contrast, co-administration of THC+CBD induced a significant anxiolytic effect, with rats spending significantly greater time in the centre zone relative to VEH ($p = 0.008$) and THC ($p < 0.001$) groups, indicating that intra-vHipp THC+CBD co-administration engenders opposite effects on anxiety relative to THC.

Given that intra-vHipp THC potently increases pERK1-2 activation (Figure 1a), we next challenged the anxiogenic effects of intra-vHipp THC with co-administration of the MEK 1-2 inhibitor, U0126. One-way ANOVA comparing VEH (n=11), THC (100 ng; n=12), and 100 ng THC+U0126 (0.1 and 1 μg; n's=8) revealed a significant main effect of Group [$F_{(3, 35)} = 3.36$, $p = 0.03$]. Post-hoc comparisons using Fisher's LSD revealed that rats receiving THC with a lower dose of U0126 (0.1 μg) displayed anxiogenic avoidance of the centre zone relative to VEH ($p = 0.028$). In contrast, rats receiving co-administration of 100 ng THC with a higher dose of U0126 (1 μg) spent significantly more time in the centre zone relative to THC ($p = 0.046$). Thus, blockade of MEK1-2 signaling dose-dependently blocks the anxiogenic effects of intra-vHipp THC, consistent with its ability to prevent intra-vHipp pERK1-2 activation.

Given our finding that activation of ERK1-2 with EPA reverses the combinatorial effects of THC+CBD on THC-induced pERK1-2 expression levels, we next challenged the anxiolytic effects of THC+CBD on centre zone times by co-administration of THC+CBD+EPA. One-way ANOVA comparing VEH (n=11), 100 ng THC+CBD (n=8), and 100 ng THC+CBD+EPA (0.1, and 1 mM; n=9, n=8, respectively) revealed a significant main effect of Group [$F_{(3, 32)} = 7.79$, $p < 0.001$]. Post-hoc comparisons using Fisher's LSD revealed that rats receiving THC+CBD with a higher dose of EPA (1 mM) spent significantly

less time in the centre zone relative to VEH ($p = 0.032$), demonstrating that vHipp ERK phosphorylation dose-dependently attenuates the anxiolytic properties of THC+CBD. A separate one-way ANOVA comparing 1 μg U0126, and 1 mM EPA (n's=8) alone with the VEH group revealed no significant main effect of Group [$F_{(2, 25)} = 3.058$, $p > 0.05$]. Representative activity plots for selected groups are presented in **Figure 2c**.

We next assessed the effects of intra-vHipp THC/CBD using the light-dark box anxiety test (portrayed in **Figure 2d**). **Figure 2e** represents the mean % time spent in the light environment between drug treatment conditions. One-way ANOVA comparing VEH (n=10), 10 (n=9) and 100 ng THC (n=11), 10 (n=9) and 100 ng CBD (n=8), and 100 ng THC+CBD (n=8) groups revealed a significant main effect of Group [$F_{(5, 49)} = 4.76$, $p = 0.001$]. Post-hoc comparisons using Fisher's LSD demonstrate dose-dependent effects of THC, as 10 ng THC increases time spent in the light compartment relative to 100 ng THC ($p < 0.001$), while 100 ng THC reduces this measure relative to 100 ng CBD ($p = 0.008$) and co-administered THC+CBD ($p < 0.001$). Although CBD displays no significant effects, THC+CBD co-administration increases time spent in the light environment compared to VEH ($p = 0.008$), indicating an anxiolytic effect that counteracts the effect of THC.

We next challenged the anxiogenic effects of intra-vHipp THC with co-administration of the MEK 1-2 inhibitor, U0126. One-way ANOVA comparing VEH (n=10), 100 ng THC (n=11), and 100 ng THC+U0126 (0.1 and 1 μg; n=9, n=8, respectively) revealed no significant main effect of Group [$F_{(3, 34)} = 1.68$, $p > 0.05$]. However, a planned pre-hoc comparison revealed significantly increased % time spent in the light environment by the 100 ng THC+1 μg U0126 group relative to THC alone [$t_{(18)} = -2.57$, $p = 0.01$]. Thus, blockade of MEK1-2 signaling dose-dependently mitigates the anxiogenic effects of intra-vHipp THC.

Next, we challenged the behavioural effects of our THC+CBD combination on % time spent in the light environment by co-administration of THC+CBD+EPA. One-way ANOVA comparing VEH (n=10), 100 ng THC+CBD (n=8), and 100 ng THC+CBD+EPA (0.1 and 1 mM; n=7, n=9, respectively) revealed a significant main effect of Group [$F_{(3, 30)} = 3.05$, $p = 0.044$]. Post-hoc comparisons using Fisher's LSD revealed that whereas rats receiving THC+CBD with a lower dose of EPA (0.1 mM) did not differ from THC+CBD, rats receiving THC+CBD with a higher dose of EPA (1 mM) spent significantly less time in the light environment ($p = 0.009$), demonstrating that vHipp pERK1-2 activation dose-dependently attenuates the anxiolytic properties of THC+CBD. A separate one-way ANOVA comparing 1 μg U0126, and 1 mM EPA (n's=8) alone with the VEH group revealed no significant main effect of Group [$F_{(2, 25)} = 0.043$, $p > 0.05$] on % time spent in the light environment.

Figure 2f represents the mean latency to initial re-emergence from the dark to light environment. One-way ANOVA comparing VEH, THC (10 and 100 ng), CBD (10 and 100 ng), and THC+CBD (100 ng) revealed a significant main effect of Group [$F_{(5\ 49)} = 3.60$, $p = 0.008$]. Post-hoc comparisons using Fisher's LSD demonstrate that the 100 ng THC group shows increased latency to re-emerge into the light environment relative to VEH ($p = 0.006$), 100 ng CBD ($p = 0.011$) and THC+CBD ($p = 0.007$). Thus, intra-vHipp THC dose-dependently increases anxiogenic avoidance behaviours that is reversed by CBD co-administration.

Comparing groups treated with VEH, 100 ng THC, and 100 ng THC+U0126 (0.1 and 1 μg), one-way ANOVA revealed a significant main effect of Group [$F (3, 34) = 4.88$, $p = 0.006$]. Post-hoc comparisons revealed that rats receiving THC with a higher dose of U0126 (1 μg) displayed significantly less latency to re-emerge into the light environment relative to

481 THC alone ($p < 0.001$) and displayed comparable latency to VEH controls. Thus, blockade of
482 intra-vHipp MEK1-2 signaling dose-dependently inhibits THC-induced anxiogenic avoidance
483 of a light environment. Furthermore, comparing the 1 μg U0126, and 1 mM EPA (n's=8)
484 alone groups with the VEH group using one-way ANOVA revealed no significant main effect
485 of Group [$F_{(2, 25)} = 0.046$, $p > 0.05$] on latency to re-emerge into the light environment.
486
487 ***Intra-vHipp THC and CBD differentially modulate contextual fear memory formation***
488 ***via local ERK1-2 modulation***
489 Considering our findings that intra-vHipp THC/CBD opposingly modulate anxiety-
490 related behaviours, we next examined whether THC/CBD could modify the aversive valence
491 of fear memory acquisition using sub-threshold footshock conditioning levels (0.4 mA). A
492 sample microphotograph of a representative vHipp microinfusion site is shown in **Figure 3a**.
493 First, using a context-dependent fear conditioning assay (see methods), we compared mean
494 % time freezing during fear memory testing (**Figure 3b**). One-way ANOVA comparing VEH
495 (n=11), 10 (n=8) and 100 ng THC (n=9), 10 (n=7) and 100 ng CBD (n=8), and 100 ng
496 THC+CBD (n=8) groups revealed a significant main effect of Group [$F_{(5, 45)} = 3.09$, $p =$
497 0.018]. Post-hoc comparisons using Fisher's LSD revealed dose-dependent effects of THC,
498 with the higher dose of THC (100 ng) inducing a significant elevation in % time freezing
499 relative to VEH ($p = 0.003$), 100 ng CBD ($p = 0.038$) and THC+CBD ($p = 0.001$). Thus,
500 whereas THC strongly potentiates the aversive salience of contextual cues linked with sub-
501 threshold footshock, THC+CBD co-administration mitigates these effects.
502 Based upon dose-response curves obtained in our anxiety-based assays, we
503 selected co-infusion doses of 1 μg U0126, and 1 mM EPA to challenge the effects of THC,

and THC+CBD on fear responsivity, respectively. One-way ANOVA comparing VEH (n=11), 100 ng THC (n=9), and 100 ng THC+U0126 (n=9) groups revealed a significant main effect of Group [$F_{(2, 26)} = 4.18$, $p = 0.027$]. Post hoc comparisons using Fisher's LSD revealed that co-administered 100 ng THC+U0126 reduced % time spent freezing relative to 100 ng THC ($p = 0.034$), demonstrating that MEK1-2 blockade counteracts THC-induced potentiation of fear responsivity.

We next challenged the antagonistic effect of intra-vHipp THC+CBD co-administration by co-infusing THC+CBD+EPA. One-way ANOVA comparing VEH (n=11), 100 ng THC+CBD (n=8), and 100 ng THC+CBD+1 mM EPA (n=10) revealed no significant main effect of Group [$F_{(2, 26)} = 2.91$, $p > 0.05$]. However, a planned pre-hoc comparison revealed that THC+CBD+EPA co-administration significantly increased % time spent freezing relative to THC+CBD [$t_{(16)} = -2.19$, $p = 0.043$], demonstrating that vHipp pERK1-2 up-regulation mitigates relief of fear-responsivity by THC+CBD. In addition, a separate one-way ANOVA comparing 1 μg U0126, and 1 mM EPA alone (n's=8) relative to VEH revealed no significant main effect of Group [$F(2, 24) = 2.71$, $p > 0.05$].

THC and CBD differentially regulate context-independent fear memory processing via interactions with ERK1-2 signaling in the vHipp

Considering that the vHipp has previously been implicated in context-independent associative memory formation (Kramar et al., 2017), we next tested the effects of intra-vHipp THC/CBD administration and the impact of pERK1-2 signaling on olfactory-cue fear memory formation using a subthreshold fear conditioning protocol (see methods). Based upon dose-response curves obtained in our context-dependent fear conditioning task (Figure 3b), we

selected doses of 100 ng THC, 100 ng CBD, and 100 ng THC+CBD for intra-vHipp microinfusions. The mean % time freezing to CS- and CS+ presentations during testing are represented in **Figure 3c**. Mixed measures ANOVA comparing VEH, THC, CBD, and THC+CBD groups (n's=8) revealed a significant main effect of Group [$F_{(3, 28)} = 13.36$, $p < 0.001$], and a significant main effect of Conditioned Stimulus Factor [$F_{(1, 28)} = 24.67$, $p < 0.001$], but not an interaction between Group and Conditioned Stimulus Factors. Post-hoc comparisons using Fisher's LSD revealed that THC significantly increases % time freezing to CS- and CS+ relative to VEH ($p = 0.022$; $p < 0.001$), CBD ($p = 0.007$; $p < 0.001$), and THC+CBD ($p = 0.007$; $p < 0.001$) groups. Thus, whereas intra-vHipp THC indiscriminately potentiates fear responsivity to associative fear-conditioned cues, THC+CBD co-administration mitigates these conditioned effects.

We next examined the impact of pERK1-2 signaling on THC-induced changes in context-independent fear responsivity. Mixed measures ANOVA comparing VEH, THC, and THC+U0126 groups (n's=8) revealed significant main effects of Group [$F_{(2, 21)} = 8.11$, $p = 0.002$], and Conditioned Stimulus Factor [$F_{(1, 21)} = 13.18$, $p = 0.002$], but not an interaction between Group and Conditioned Stimulus Factors. Post-hoc comparisons using Fisher's LSD revealed that rats treated with THC+U0126 display less % time freezing to the CS+ relative to THC alone ($p = 0.004$), and do not differ in CS- freezing % relative to VEH. Thus, inhibition of pERK1-2 signaling is sufficient to counteract THC-induced potentiation of fear responsivity.

Next, we examined the potential role of pERK1-2 signaling in the inhibitory action of CBD co-administration on THC-induced fear responsivity by co-administering THC+CBD+EPA. Mixed measures ANOVA comparing VEH, THC+CBD, and

THC+CBD+EPA groups (n's=8) revealed significant main effects of Group [$F_{(2, 21)}$ = 10.61, p < 0.001], and Conditioned Stimulus Factor [$F_{(1, 21)}$ = 28.54, p < 0.001], but no interaction between Group and Conditioned Stimulus Factors. Post-hoc comparisons indicated co-infusion of THC+CBD+EPA increased % time freezing to CS- and CS+ relative to THC+CBD (p = 0.026; p < 0.001), indicating that CBD co-administration rescues THC-induced associative fear memory formation via inhibition of vHipp pERK1-2 activation. Additionally, a separate mixed measures ANOVA comparing 1 μg U0126, and 1 mM EPA alone (n's=8) relative to VEH revealed a significant main effect of Conditioned Stimulus Factor [$F_{(1, 21)}$ = 10.25, p = 0.004], but no significant main effect of Group or interaction between Group and Conditioned Stimulus Factors.

Intra-vHipp THC and CBD produce opposite effects on opioid reward processing via local ERK1-2 modulation

In addition to modulation of fear-related associative memory, using a morphine-dependent place conditioning procedure (CPP), we recently reported that vHipp CB1R activation can strongly potentiate opioid reward memory salience (Loureiro et al., 2015). Therefore, we used a sub-reward threshold conditioning doses of morphine (0.05 mg/kg, i.p.) with an unbiased CPP design (see methods) assessing mean % time spent in the morphine-paired and saline-paired contexts during CPP testing (**Figure 3d**). Mixed measures ANOVA comparing VEH, THC, CBD, and THC+CBD groups (n's=7) revealed a significant interaction between Group and Context Factors [$F_{(3, 24)}$ = 3.38, p = 0.035], but no significant main effect of Group, or Context Factor. Post-hoc comparisons using Fisher's LSD indicated that THC significantly increased % time spent in the morphine context relative to VEH (p = 0.035),

CBD ($p = 0.028$), and THC+CBD ($p = 0.007$) groups. Furthermore, a planned pre-hoc comparison revealed that rats receiving THC+CBD co-administration demonstrated greater % time spent in the saline vs. morphine-paired contexts [$t_{(12)} = -1.93$, $p = 0.039$]. Thus, whereas intra-vHipp THC potentiates the reward salience of morphine, THC+CBD co-administration reverses this effect, producing aversion to morphine-paired contexts. We also separately analyzed both the average time spent in the centre grey compartment (one-way ANOVA: [$F(3, 24) = 1.39$, $p > 0.05$]), as well as the average time spent in either conditioning environment (mixed measures ANOVA: [$F(3, 48) = 0.68$, $p > 0.05$]) to examine possible contextual bias, but the analyses revealed no significant differences between groups.

We next examined whether the ability of intra-vHipp THC to modulate morphine-dependent reward processing may depend upon local pERK1-2 signaling. Mixed measures ANOVA comparing VEH, THC, and THC+U0126 (n=8) groups revealed a significant interaction between Group and Context [$F_{(2, 19)} = 4.02$, $p = 0.035$]. Post-hoc comparisons using Fisher's LSD showed that rats receiving THC+U0126 did not differ from VEH in % time spent in the morphine context, suggesting that THC potentiates the rewarding properties of morphine via local pERK1-2 signaling. We also assessed the role of pERK1-2 signaling on the opposing actions of THC+CBD on CPP via co-administration of THC+CBD+EPA. Mixed measures ANOVA comparing VEH, THC+CBD, and THC+CBD+EPA groups (n's=7) revealed a significant main effect of Group [$F_{(2, 18)} = 4.24$, $p = 0.031$]. Post-hoc comparisons indicated that relative to rats receiving VEH ($p = 0.022$), those receiving THC+CBD+EPA increased % time spent in the morphine context. Therefore, CBD co-administration reverses the potentiation of reward memory salience induced by intra-vHipp THC via local pERK1-2 inhibition.

THC, CBD, and their combination enhance preference for a low-concentration sucrose solution

We next examined the effects of THC, CBD, and their combination on responses toward a natural reward using the sucrose preference assay (see methods). Mean preference for 2% sucrose solution is represented in **Figure 3e**. One-way ANOVA comparing VEH (n=7), THC (n=8), CBD (n=7), and THC+CBD (n=7; 100 ng each) revealed a significant main effect of Group [$F_{(3, 25)} = 5.61$, $p = 0.004$], and post-hoc comparisons using Fisher's LSD revealed that THC ($p = 0.001$), CBD ($p = 0.002$), and THC+CBD ($p = 0.01$) each significantly increase sucrose preference compared to VEH. Similar results were observed when comparing water intake between groups during the sucrose preference assay (main effect of Group [$F_{(3, 25)} = 4.51$, $p = 0.012$]; **Figure 3f**). Total caloric intake during testing did not differ between groups ([$F_{(3, 25)} = 2.48$, $p = 0.084$]). Thus, intra-vHipp THC, CBD, and combined THC+CBD each selectively enhance preference for a low-concentration sucrose reward by decreasing water intake, without altering total caloric consumption or food intake.

Intra-vHipp THC elicits a hyperactive VTA DA activity state via ERK1-2 activation and is blocked by CBD

We next performed intra-VTA extracellular single-unit recordings to determine if VTA DA neuronal activity states are modulated by intra-vHipp VEH (cells/animals; n=13/5), THC (n=19/6), CBD (n=12/4), combined THC+CBD (n=16/6), or local pERK1-2 activity using THC+U0126 (n=14/5). Sample microphotographs of a representative vHipp microinfusion

location and VTA neuronal recording site are shown in **Figure 4a-b**. Neuronal activity profiles following intra-vHipp microinfusion treatments are summarized in **Figure 4c**. **Figure 4d** represents mean frequency change (expressed as % relative to baseline) in VTA DA neurons, and one-way ANOVA revealed a significant main effect of Group [$F_{(4, 69)}$ = 3.54 p = 0.011]. Post-hoc comparisons using Newman Keuls' test revealed that VTA DA neuronal firing frequencies were significantly increased following intra-vHipp THC relative to VEH (p = 0.028), CBD (p < 0.001), THC+CBD (p = 0.011) groups. One-way ANOVA comparing mean VTA DA bursting activity change (expressed as bursts/min, % relative to baseline) between VEH (cells/animals; n=11/5), THC (n=14/6), CBD (n=10/4), THC+CBD (n=16/6), and THC+U0126 (n=11/5) revealed similar results (significant main effect of Group [$F_{(4, 57)}$ = 2.61, p = 0.045]; **Figure 4e**). Thus, whereas THC increases VTA DA neuronal frequency and phasic bursting rates through a vHipp pERK1-2 dependent substrate, THC+CBD co-administration mitigates these changes. Rastergrams demonstrating effects on firing frequency according to treatment with THC alone, or combined THC+CBD are represented in **Figure 4f-g**, respectively.

Intra-vHipp THC and CBD reduce VTA non-DA neuronal activity

Putative non-DA neurons isolated in the VTA were also analyzed. Neuronal activity profiles following intra-vHipp microinfusion treatments are summarized in **Figure 5a**. **Figure 5b** represents mean frequency change (expressed as % relative to baseline) in VTA non-DA neurons. One-way ANOVA comparing VEH (cells/animals, n=15/5), THC (n=14/6), CBD (n=11/4), THC+CBD (n=11/6), and THC+U0126 groups (n=14/5) revealed a significant main effect of Group [$F_{(4, 60)}$ = 3.01, p = 0.025]. Post-hoc comparisons using Newman Keuls' test

reveal that THC ($p = 0.008$) and CBD ($p = 0.041$) each reduce VTA non-DA neuronal frequency rates relative to VEH. Co-administration of THC+CBD ($p= 0.007$), and THC+U0126 ($p = 0.019$) each mitigated the actions of THC. Rastergrams demonstrating effects on firing frequency according to treatment with THC alone, or combined THC+CBD are shown in **Figure 5c-d**, respectively.

Intra-vHipp THC and CBD exert distinct control over VTA oscillatory frequencies

Local field potential (LFP) recordings in the VTA were obtained simultaneously with single-unit activity. The strength of the oscillations was assessed by calculating power spectral densities (PSD; window length=2 s; shift=0.5 s) during the 5-minute pre-infusion and post-infusion recording epochs, averaging PSDs within epochs and subsequently normalizing the averaged PSD to the total power (normalized total power=1; frequencies values between 59-61 Hz were excluded to avoid contamination with 60 Hz noise from power line). **Figure 6a** depicts representative VTA spectrograms in the pre- and post-infusion recording epochs following intra-vHipp microinfusions of 100 ng THC, and **Figure 6b** represents the average normalized power spectra corresponding to VTA LFP of rats receiving VEH or THC. Difference scores calculated between pre- and post-infusion epochs for β, γ, and ε power spectra oscillations, calculated as the sum of power values for frequencies between 15-30 Hz, 30-80 Hz, and 90-100 Hz respectively, following infusion of VEH (n=16), THC (n=15), CBD (n=16), THC+CBD (n=15), and THC+U0126 (n=12) are represented in **Figure 6c-e**.

One-way ANOVA examining oscillatory power changes in the β frequency range upon intra-vHipp THC revealed a significant main effect of Group [$F_{(4, 69)} = 6.70$, $p < 0.001$],

and post-hoc comparisons using Newman Keuls' test show that THC significantly increases β power relative to all other groups ($p < 0.001$ for all). Comparable results are observed within γ, and ε frequency ranges (γ: main effect of Group [$F_{(4, 69)} = 5.22$, $p < 0.001$]; ε: main effect of Group [$F_{(4, 69)} = 2.99$, $p = 0.024$]). These data suggest that local pERK1-2 activation regulates THC-induced dysregulation of intra-VTA β, γ, and ε frequencies, consistent with the observed VTA neuronal frequency abnormalities induced by THC.

Discussion

Emerging evidence suggests that CBD possesses antipsychotic properties and can mitigate many of the psychotropic side-effects of THC (Bhattacharyya et al., 2010; Renard et al., 2016a). Cannabis strains and extracts containing high-THC and low-CBD concentrations are linked to increased neuropsychiatric risk (Beale et al., 2018; Di Forti et al., 2009; Englund et al., 2013; Schubart et al., 2011), underscoring the importance of CBD as a mitigating factor in reducing THC-related neuropsychiatric side-effects. However, little is understood regarding how CBD produces these mitigating effects at the neuronal, molecular and behavioural levels. We report that intra-vHipp THC increases VTA DA frequency and bursting rates while concomitantly decreasing GABAergic neuronal activity, and increasing the magnitude of intra-VTA β, γ, and ε oscillatory frequencies via a vHipp pERK1-2 mediated mechanism. Whereas THC induces an anxiogenic phenotype and distorts reward and aversion-related salience attribution, we found that THC+CBD co-administration blocked these effects through differential modulation of local vHipp pERK1-2 signaling states.

Consistent with evidence linking hippocampal CB1R stimulation with pERK1-2 activation (Derkinderen et al., 2003), we observed strongly upregulated local pERK1-2

expression following intra-vHipp THC administration. This effect was selectively blocked by co-administration of the MEK1-2 inhibitor, U0126. Although CBD alone produced no effect on pERK1-2 expression, co-administered THC+CBD reversed the effects of THC and significantly downregulating pERK1-2 expression relative to THC and VEH groups. This is the first evidence, to our knowledge, that combined THC+CBD functionally reverses the actions of THC on local pERK1-2 signaling. Given that CBD modulates ERK signaling through a very narrow dose range (Solinas et al., 2013), primarily via cannabinoid and vanilloid receptor-independent mechanisms (McPartland et al., 2007), indirect mechanisms such modulation of endocannabinoid signaling could underlie the effects by CBD on pERK1-2 activity in the current study. In addition, CBD's inhibitory effect on THC-induced pERK1-2 activation was blocked by local application of the ERK activator, EPA, further demonstrating the importance of vHipp ERK phosphorylation in the functional effects of THC and CBD. Interestingly, at the molecular level, the results of the current study resemble post-mortem assays conducted with brains of schizophrenia cohorts (Kozlovsky et al., 2004).

The ERK signal transduction cascade is a critical regulator of synaptic plasticity, DA and glutamate neurotransmission, and affective processing, each of which are dysregulated in schizophrenia and related disorders (Yuan et al., 2010). ERK expression is functionally coupled with hippocampal CB1R stimulation, which can overdrive mesolimbic DA transmission and disrupt gating of emotionally salient information (Derkinderen et al., 2003; Loureiro et al., 2015). Given that vHipp CB1Rs are highly expressed on cholecystokinin (CCK)-positive GABAergic interneurons (Derkinderen et al., 2003; Takács et al., 2015), direct agonism of these CB1Rs represents one potential mechanism driving THC-induced pERK1-2 activation.

Alterations in hippocampal pERK1-2 signaling are associated with exposure to stressors and anxiety behaviours, and ERK phosphorylation is importantly involved in fear-related learning and memory processing (Huh et al., 2009; Ritov et al., 2014; Selcher et al., 2003). Thus, our findings that vHipp THC induces a dramatic increase in local ERK1-2 phosphorylation states suggests a potential molecular mechanism by which THC might serve to amplify the salience of incoming affective contextual stimuli. Indeed, distortions of fear-related associative memory are observed following THC administration in the nucleus accumbens (Fitoussi et al., 2018) and also upon CB1R stimulation in the vHipp or basolateral nucleus of the amygdala (Laviolette and Grace, 2006; Loureiro et al., 2015). Activation of vHipp CB1Rs reduce local GABA release, thereby increasing hippocampal excitatory output (Ha´jos and Freund, 2002; Ivanov et al., 2006), and the psychotomimetic effects of THC in both humans and rodents have been shown to be directly related to striatal glutamate influx (Colizzi et al., 2019; Loureiro et al., 2015).

Behaviourally, we observed dose-dependent, biphasic modulation of anxiety behaviours following intra-vHipp THC. Previous evidence has suggested that the anxiolytic and anxiogenic effects of low- vs high-dose CB1R agonists are independently modulated by activation of CB1Rs expressed on glutamatergic vs GABAergic neuronal populations (Aparisi Rey et al., 2012). Furthermore, hippocampal CB1Rs are expressed at greater concentrations on GABAergic interneurons relative to glutamatergic neurons (Marsicano and Lutz, 1999; Nyiri et al., 2005; Takács et al., 2015) with CB1R activation preferentially targeting GABA interneurons (Pertwee, 2005; Roberto et al., 2010). These cell-specific differences could explain the differential anxiolytic-like vs anxiogenic-like effects of low-dose vs high dose THC, via saturation of CB1Rs localized on vHipp glutamatergic vs GABAergic neurons,

734 respectively. While CBD had no effect alone, combined THC+CBD reversed THC-induced
735 anxiogenesis, which was blocked by activation of vHipp pERK1-2 signaling, emphasizing the
736 functional role of vHipp pERK1-2 inhibition in the anxiolytic properties of CBD. Thus, THC
737 and CBD exert opposing control over anxiety-related behavioural responses via differential
738 regulation of vHipp ERK phosphorylation.

739 Hippocampal ERK activation is critically involved in fear-related associative learning
740 (Huh et al., 2009; Ritov et al., 2014; Selcher et al., 2003), and is necessary for reward-
741 related and hippocampal-dependent memory formation (Berman et al., 1998; Besnard et al.,
742 2013). In the current study, we found that intra-vHipp THC potentiated the rewarding
743 properties of a normally sub-reward threshold conditioning dose of morphine and also
744 amplified conditioned fear responses to context-dependent and context-independent cues.
745 Both effects were blocked by MEK 1-2 inhibition or by CBD co-administration. These effects
746 are consistent with changes in affective memory formation observed following acute vHipp
747 CB1R, and GPR55 stimulation (Kramar et al., 2017; Loureiro et al., 2015), and support the
748 hypothesis that THC dysregulates vHipp excitatory output leading to aberrant emotional
749 sensory processing. Genetic variations of both the Akt and DA transporter genes are
750 associated with dysregulation of DA signaling within the striatum and mesolimbic circuitry, as
751 well as psychosis following acute, high dose THC exposure (Colizzi et al., 2019; Morgan et
752 al., 2016). Intriguingly, we also observed a THC-specific generalization of fear responding to
753 olfactory CS- within context-independent fear testing, suggesting that intra-vHipp THC
754 disrupts salience attribution toward affective sensory stimuli. The current design does not
755 allow us to speculate as to whether this result is due to generalization of conditioned
756 stimulus processing vs generalized negative affect. However, previous evidence suggests

that CBD regulates fear-related memory processing by disrupting fear memory consolidation and enhancing fear extinction, both of which can result in a lasting reduction of learned fear (Lee et al., 2017; Norris et al., 2016), possibly underlying the mitigation of fear-responsivity following THC+CBD co-administration. Thus, similar to effects observed in anxiety-like behaviours, the combination of THC+CBD is capable of counteracting THC-induced affective memory changes by blocking THC-induced local ERK 1-2 activation.

Interestingly, THC, CBD, and their combination each increased natural, sucrose-related appetitive behaviours, suggesting that CBD-related mitigation of affective motivation may be selective for drug-related (vs. natural) reward cues. Although CBD engendered few behavioural changes in the current study, changes in sucrose preference by systemic CBD administration is a well-established phenomenon (Bisogno et al., 2001; Park et al., 2008). The precise mechanism of action of CBD remains unknown, previous evidence largely excludes cannabinoid and vanilloid receptor contributions (Bisogno et al., 2001), and we have previously demonstrated the involvement of 5-HT1ARs in CBD-induced mitigation of emotional memory expression (Norris et al., 2016). Although CBD does not seem to have marked effects on any relevant physiological or symptomatic variables under normal circumstances (Martin-Santos et al., 2012), it appears to exert powerful modulation over cue-induced responsivity in associative learning tasks and in those with compromised neuropsychiatric statuses (Devinsky et al., 2014; Ren et al., 2009).

Through control of DA neuronal activity states, the vHipp relays affective-contextual information to downstream limbic regions. vHipp dysfunction may underlie DA dysregulation in schizophrenia, leading to impairments in salience attribution toward affective stimuli. For example, vHipp stimulation increases the number of spontaneously active VTA DA neurons

and striatal DA influx (Floresco et al., 2001; Legault et al., 2000), and the psychotomimetic effects of THC are directly related to striatal DA and glutamate levels (Bhattacharyya et al., 2012; Colizzi et al., 2019; Fitoussi et al., 2018). Using *in vivo* single-cell electrophysiological recordings, we found that intra-vHipp THC significantly increased both frequency and bursting rates of VTA DA neurons. Interestingly, although CBD alone had no effect, co-infusion of THC+CBD, or THC+U0126 reversed THC-induced DA hyperactivity, demonstrating the direct involvement of vHipp ERK signaling in these effects.

Changes in VTA DA activity patterns from tonic to phasic burst firing are associated with phasic DA release in the nucleus accumbens, which encodes unexpected outcomes, such as prediction errors. Acute or neurodevelopmental THC exposure has been shown to induce a hyperactive mesolimbic DA state, both in terms of increased frequency and bursting in VTA DAergic neuronal populations (Fitoussi et al., 2018; Renard et al., 2017). CB1Rs are predominantly expressed presynaptically on GABAergic axon terminals within the hippocampus and recent studies reveal that THC exhibits full agonist efficacy at these CB1Rs (Laaris et al., 2010; Marsicano and Lutz, 1999; Nyiri et al., 2005), possibly accounting for the hyperactive VTA DA endophenotype observed in our current study. They may also be relevant for interpreting the actions of the THC+CBD combination; given that CBD increases endocannabinoid tone (Leishman et al., 2018), co-administered THC+CBD may indirectly antagonise the actions of THC on CB1Rs in the vHipp. Consistent with evidence that hippocampal ERK signaling facilitates generation of DAergic neuronal prediction errors (Huh et al., 2009), and that CBD normalizes VTA DA activity (Renard et al., 2016a), co-infusion of CBD, or the MEK1-2 inhibitor U0126 each prevented the THC-induced increase in VTA DA phasic bursting. Although VTA DA vs non-DA neurons are well-

characterised and display canonical activity profiles in-vivo, it has been previously demonstrated that a subset of tyrosine hydroxylase-positive VTA neurons display alternative physiological properties, and that no physiological property is both sensitive and selective for DA vs GABAergic neurons in the VTA (Margolis et al., 2006). Thus, it is important to recognize that the features used to characterise neuronal sub-populations in the current study are not ubiquitous.

In schizophrenia, loss of hippocampal GABAergic activity is hypothesized to disinhibit hippocampal outputs, inducing a hyperdopaminergic state (Grace, 2010). Reductions in PV-expressing interneurons are reliably observed in schizophrenia patients and are linked to NMDA receptor desensitization (Gonzalez-Burgos and Lewis, 2012). Similar aberrant volumetric deficits and physiological changes are observed in chronic cannabis users (Beale et al., 2018). Importantly, these local interneurons are necessary for the generation of normal γ oscillations (Benes et al., 2007). In the VTA, LFPs are comprised of integrated input from several structures, including the hippocampus, nucleus accumbens and mPFC (Cembrowski et al., 2018). Considerable evidence demonstrates that dysregulated γ oscillations contribute to schizophrenia-related perceptual and cognitive deficits (Baldeweg et al., 1998). γ oscillations crucially subserve high-frequency oscillations (HFO), including ε, and frequently couple with slower frequencies, including β (Buzsáki et al., 2012). HFOs, including epsilon, are evoked following hippocampal stimulation and coincide with excitotoxicity and seizure-like discharges (Fisher et al., 1992). Intriguingly, it has been suggested that β and γ frequency ranges may be particularly involved in long-range neural coordination (Kopell, 2000), and may underlie schizophrenia-related dysfunctional connectivity among cortical and subcortical networks. We observed increased oscillatory

826 frequency in VTA beta, gamma, and epsilon power following intra-vHipp THC. In contrast,
827 although CBD alone had no effect alone, co-infusion of CBD, or the MEK1-2 inhibitor U0126,
828 each counteracted these THC-induced effects on VTA oscillations suggesting functional
829 involvement of vHipp ERK signaling in these oscillatory effects.

830 CB1R agonists dysregulate hippocampal and cortical beta and gamma magnitudes
831 to a similar extent to that observed in schizophrenia (Cass et al., 2014; Morrison et al., 2011;
832 Renard et al., 2017). However, no studies to date have examined these effects directly in the
833 VTA. Evidence suggests that CBD restores membrane excitability in PV- and CCK-
834 expressing cells (Campos et al., 2013; Drysdale et al., 2006; Khan et al., 2018), suggesting
835 that CBD co-administration may restore vHipp inhibitory control to counteract the neural
836 effects of THC. That said, across several behavioural and electrophysiological measures, the
837 effects of THC+CBD are different than those observed for vehicle alone, and in the opposite
838 direction of THC. In other cases, CBD and THC each produce similar effects (see Fig. 3e-f).
839 It is important to note that the pharmacodynamic and pharmacokinetic mechanisms by which
840 THC and CBD exert their effects are complicated, and become even more intricate when
841 delivered in combination (Russo, 2011). Thus, it is not always possible to attribute the
842 actions of the THC+CBD combination to one proposed molecular mechanism. Despite
843 feasibility limitations and although outside of the scope of the present study, examining the
844 actions of CBD+EPA, or THC+EPA may have aided interpretation across several measures.
845 Given that interactions between hippocampal CB1R activation and ERK phosphorylation
846 critically regulate DA neurotransmission and maintenance of normal oscillatory activity, the
847 present findings provide further evidence for the contrasting effects of intra-vHipp THC/CBD
848 on VTA oscillatory magnitudes.

In summary, the behavioural and neurophysiological disturbances elicited by intra-vHipp THC mimic a range of neuropsychiatric symptoms resembling core endophenotypes of schizophrenia. The present findings identify a common mechanism by which distinct phytocannabinoids may differentially modulate neuropsychiatric side-effects of cannabis exposure through the bi-directional control of localized hippocampal ERK 1-2 phosphorylation states, mesolimbic DA activity levels and associated oscillatory wave patterns.

Authorship Contributions

R.H. contributed to the conception and design, data acquisition and analyses, interpretation of results, and drafted the manuscript. J.R. H.S. and C.N. contributed to data analysis and interpretation of results. W.J.R. and S.R.L. contributed to the conception and design of experiments, interpretation of results, and manuscript draft.

872 **References**

873 Baldeweg T, Spence S, Hirsch SR, Gruzelier J (1998) γ-band electroencephalographic
874 oscillations in a patient with somatic hallucinations. The Lancet 352:620-621.
875 Beale C, Broyd SJ, Chye Y, Suo C, Schira M, Galettis P, Martin JH, Yücel M, Solowij N
876 (2018) Prolonged cannabidiol treatment effects on hippocampal subfield volumes
877 in current cannabis users. Cannabis and cannabinoid research 3:94-107.
878 Benes FM, Lim B, Matzilevich D, Walsh JP, Subburaju S, Minns M (2007) Regulation of
879 the GABA cell phenotype in hippocampus of schizophrenics and bipolars.
880 Proceedings of the National Academy of Sciences 104:10164-10169.
881 Berman DE, Hazvi S, Rosenblum K, Seger R, Dudai Y (1998) Specific and differential
882 activation of mitogen-activated protein kinase cascades by unfamiliar taste in the
883 insular cortex of the behaving rat. Journal of Neuroscience 18:10037-10044.
884 Besnard A, Caboche J, Laroche S (2013) Recall and reconsolidation of contextual fear
885 memory: differential control by ERK and Zif268 expression dosage. PLoS One
886 8:e72006.
887 Bhattacharyya S, Falkenberg I, Martin-Santos R, Atakan Z, Crippa JA, Giampietro V,
888 Brammer M, McGuire P (2015) Cannabinoid modulation of functional connectivity
889 within regions processing attentional salience. Neuropsychopharmacology
890 40:1343.
891 Bhattacharyya S, Morrison PD, Fusar-Poli P, Martin-Santos R, Borgwardt S, Winton-
892 Brown T, Nosarti C, O'Carroll CM, Seal M, Allen P (2010) Opposite effects of Δ-
893 9-tetrahydrocannabinol and cannabidiol on human brain function and
894 psychopathology. Neuropsychopharmacology 35:764.

895 Bhattacharyya S, Crippa JA, Allen P, Martin-Santos R, Borgwardt S, Fusar-Poli P,
896 Rubia K, Kambeitz J, O'carroll C, Seal ML (2012) Induction of psychosis byδ9-
897 tetrahydrocannabinol reflects modulation of prefrontal and striatal function during
898 attentional salience processing. Archives of general psychiatry 69:27-36.
899 Bisogno T, Hanuš L, De Petrocellis L, Tchilibon S, Ponde DE, Brandi I, Moriello AS,
900 Davis JB, Mechoulam R, Di Marzo V (2001) Molecular targets for cannabidiol
901 and its synthetic analogues: effect on vanilloid VR1 receptors and on the cellular
902 uptake and enzymatic hydrolysis of anandamide. British journal of pharmacology
903 134:845-852.
904 Buzsáki G, Wang X-J (2012) Mechanisms of gamma oscillations. Annual review of
905 neuroscience 35:203-225.
906 Campos AC, Ortega Z, Palazuelos J, Fogaça MV, Aguiar DC, Díaz-Alonso J, Ortega-
907 Gutiérrez S, Vázquez-Villa H, Moreira FA, Guzmán M (2013) The anxiolytic effect
908 of cannabidiol on chronically stressed mice depends on hippocampal
909 neurogenesis: involvement of the endocannabinoid system. International Journal
910 of Neuropsychopharmacology 16:1407-1419.
911 Cass DK, Flores-Barrera E, Thomases DR, Vital WF, Caballero A, Tseng KY (2014)
912 CB1 cannabinoid receptor stimulation during adolescence impairs the maturation
913 of GABA function in the adult rat prefrontal cortex. Molecular psychiatry 19:536.
914 Cembrowski MS, Wang L, Lemire AL, Copeland M, DiLisio SF, Clements J, Spruston N
915 (2018) The subiculum is a patchwork of discrete subregions. eLife 7:e37701.
916 Colizzi, M., Weltens, N., McGuire, P., Lythgoe, D., Williams, S., Van Oudenhove, L., &
917 Bhattacharyya, S. (2019). Delta-9-tetrahydrocannabinol increases striatal

glutamate levels in healthy individuals: implications for psychosis. Molecular psychiatry, 1.

Derkinderen P, Valjent E, Toutant M, Corvol J-C, Enslen H, Ledent C, Trzaskos J, Caboche J, Girault J-A (2003) Regulation of extracellular signal-regulated kinase by cannabinoids in hippocampus. Journal of Neuroscience 23:2371-2382.

Devinsky, O., Cilio, M. R., Cross, H., Fernandez-Ruiz, J., French, J., Hill, C., ... & Martinez-Orgado, J. (2014). Cannabidiol: pharmacology and potential therapeutic role in epilepsy and other neuropsychiatric disorders. Epilepsia, 55(6): 791-802.

Di Forti M, Morgan C, Dazzan P, Pariante C, Mondelli V, Marques TR, Handley R, Luzi S, Russo M, Paparelli A (2009) High-potency cannabis and the risk of psychosis. The British Journal of Psychiatry 195:488-491.

Drysdale AJ, Ryan D, Pertwee RG, Platt B (2006) Cannabidiol-induced intracellular Ca2+ elevations in hippocampal cells. Neuropharmacology 50:621-631.

Duncia, J. V., Santella III, J. B., Higley, C. A., Pitts, W. J., Wityak, J., Frietze, W. E., ... & Teleha, C. A. (1998). MEK inhibitors: the chemistry and biological activity of U0126, its analogs, and cyclization products. Bioorganic & medicinal chemistry letters, 8(20), 2839-2844.

Elbaz M, Nasser MW, Ravi J, Wani NA, Ahirwar DK, Zhao H, Oghumu S, Satoskar AR, Shilo K, Carson III WE (2015) Modulation of the tumor microenvironment and inhibition of EGF/EGFR pathway: Novel anti-tumor mechanisms of Cannabidiol in breast cancer. Molecular oncology 9:906-919.

Englund A, Morrison PD, Nottage J, Hague D, Kane F, Bonaccorso S, Stone JM, Reichenberg A, Brenneisen R, Holt D (2013) Cannabidiol inhibits THC-elicited

941 paranoid symptoms and hippocampal-dependent memory impairment. Journal of
942 Psychopharmacology 27:19-27.
943 Fisher RS, Webber W, Lesser RP, Arroyo S, Uematsu S (1992) High-frequency EEG
944 activity at the start of seizures. Journal of clinical neurophysiology: official
945 publication of the American Electroencephalographic Society 9:441-448.
946 Fitoussi A, Zunder J, Tan H, Laviolette SR (2018) Delta-9-tetrahydrocannabinol
947 potentiates fear memory salience through functional modulation of mesolimbic
948 dopaminergic activity states. European Journal of Neuroscience 47:1385-1400.
949 Floresco SB, Todd CL, Grace AA (2001) Glutamatergic afferents from the hippocampus
950 to the nucleus accumbens regulate activity of ventral tegmental area dopamine
951 neurons. Journal of Neuroscience 21:4915-4922.
952 Gomes FV, Issy AC, Ferreira FR, Viveros M-P, Del Bel EA, Guimarães FS (2015)
953 Cannabidiol attenuates sensorimotor gating disruption and molecular changes
954 induced by chronic antagonism of NMDA receptors in mice. International Journal
955 of Neuropsychopharmacology 18.
956 Gonzalez-Burgos G, Lewis DA (2012) NMDA receptor hypofunction, parvalbumin-
957 positive neurons, and cortical gamma oscillations in schizophrenia.
958 Schizophrenia bulletin 38:950-957.
959 Grace A, Bunney B (1983) Intracellular and extracellular electrophysiology of nigral
960 dopaminergic neurons—1. Identification and characterization. Neuroscience
961 10:301-315.
962 Grace AA (2010) Ventral hippocampus, interneurons, and schizophrenia: a new
963 understanding of the pathophysiology of schizophrenia and its implications for

964 treatment and prevention. Current directions in psychological science 19:232-
965 237.
966 Hajós M, Hoffmann WE, Kocsis B (2008) Activation of cannabinoid-1 receptors disrupts
967 sensory gating and neuronal oscillation: relevance to schizophrenia. Biological
968 psychiatry 63:1075-1083.
969 Hájos N, Freund TF (2002) Distinct cannabinoid sensitive receptors regulate
970 hippocampal excitation and inhibition. Chemistry and Physics of Lipids 121:73-
971 82.
972 Huh KH, Guzman YF, Tronson NC, Guedea AL, Gao C, Radulovic J (2009)
973 Hippocampal Erk mechanisms linking prediction error to fear extinction: roles of
974 shock expectancy and contextual aversive valence. Learning & Memory 16:273-
975 278.
976 Ivanov A, Pellegrino C, Rama S, Dumalska I, Salyha Y, Ben-Ari Y, Medina I (2006)
977 Opposing role of synaptic and extrasynaptic NMDA receptors in regulation of the
978 extracellular signal-regulated kinases (ERK) activity in cultured rat hippocampal
979 neurons. The Journal of physiology 572:789-798.
980 Kozlovsky N, Shanon-Weickert C, Tomaskovic-Crook E, Kleinman JE, Belmaker RH,
981 Agam G (2004) Reduced GSK-3 mRNA levels in postmortem dorsolateral
982 prefrontal cortex of schizophrenic patients. J Neural Transm, 111(12): 1583–
983 1592
984 Khan AA, Shekh-Ahmad T, Khalil A, Walker MC, Ali AB (2018) Cannabidiol exerts
985 antiepileptic effects by restoring hippocampal interneuron functions in a temporal
986 lobe epilepsy model. British journal of pharmacology 175:2097-2115.

987 Kopell N, Ermentrout G, Whittington M, Traub R (2000) Gamma rhythms and beta
988 rhythms have different synchronization properties. Proceedings of the National
989 Academy of Sciences 97:1867-1872.
990 Kramar C, Loureiro M, Renard J, Laviolette SR (2017) Palmitoylethanolamide
991 modulates GPR55 receptor signaling in the ventral hippocampus to regulate
992 mesolimbic dopamine activity, social interaction, and memory processing.
993 Cannabis and Cannabinoid Research 2:8-20.
994 Laaris N, Good CH, Lupica CR (2010) Δ9-tetrahydrocannabinol is a full agonist at CB1
995 receptors on GABA neuron axon terminals in the hippocampus.
996 Neuropharmacology 59:121-127.
997 Laviolette SR, van der Kooy D (2003) Blockade of mesolimbic dopamine transmission
998 dramatically increases sensitivity to the rewarding effects of nicotine in the
999 ventral tegmental area. Molecular psychiatry 8:50.
1000 Laviolette SR, Grace AA (2006) Cannabinoids potentiate emotional learning plasticity in
1001 neurons of the medial prefrontal cortex through basolateral amygdala inputs.
1002 Journal of Neuroscience 26:6458-6468.
1003 Lee, J. L., Bertoglio, L. J., Guimarães, F. S., & Stevenson, C. W. (2017). Cannabidiol
1004 regulation of emotion and emotional memory processing: relevance for treating
1005 anxiety-related and substance abuse disorders. British journal of pharmacology,
1006 174(19), 3242-3256.
1007 Legault M, Rompré P-P, Wise RA (2000) Chemical stimulation of the ventral
1008 hippocampus elevates nucleus accumbens dopamine by activating dopaminergic
1009 neurons of the ventral tegmental area. Journal of Neuroscience 20:1635-1642.

1010 Leishman, E., Manchanda, M., Thelen, R., Miller, S., Mackie, K., & Bradshaw, H. B.
1011 (2018). Cannabidiol's Upregulation of N-acyl Ethanolamines in the Central
1012 Nervous System Requires N-acyl Phosphatidyl Ethanolamine-Specific
1013 Phospholipase D. Cannabis and Cannabinoid Research, 3(1), 228-241.
1014 Leweke F, Piomelli D, Pahlisch F, Muhl D, Gerth C, Hoyer C, Klosterkötter J, Hellmich
1015 M, Koethe D (2012) Cannabidiol enhances anandamide signaling and alleviates
1016 psychotic symptoms of schizophrenia. Translational psychiatry 2:e94.
1017 Lintas A, Chi N, Lauzon NM, Bishop SF, Gholizadeh S, Sun N, Tan H, Laviolette SR
1018 (2011) Identification of a dopamine receptor-mediated opiate reward memory
1019 switch in the basolateral amygdala–nucleus accumbens circuit. Journal of
1020 Neuroscience 31:11172-11183.
1021 Loureiro M, Renard J, Zunder J, Laviolette SR (2015) Hippocampal cannabinoid
1022 transmission modulates dopamine neuron activity: impact on rewarding memory
1023 formation and social interaction. Neuropsychopharmacology 40:1436.
1024 Loureiro M, Kramar C, Renard J, Rosen LG, Laviolette SR (2016) Cannabinoid
1025 transmission in the hippocampus activates nucleus accumbens neurons and
1026 modulates reward and aversion-related emotional salience. Biological psychiatry
1027 80:216-225.
1028 Lyons D, de Jaeger X, Rosen LG, Ahmad T, Lauzon NM, Zunder J, Coolen LM,
1029 Rushlow W, Laviolette SR (2013) Opiate exposure and withdrawal induces a
1030 molecular memory switch in the basolateral amygdala between ERK1/2 and
1031 CaMKIIα-dependent signaling substrates. Journal of Neuroscience 33:14693-
1032 14704.

1033 Maher F, Martin D, Lynch M (2004) Increased IL-1β in cortex of aged rats is
1034 accompanied by downregulation of ERK and PI-3 kinase. Neurobiology of aging
1035 25:795-806.
1036 Margolis, E. B., Lock, H., Hjelmstad, G. O., & Fields, H. L. (2006). The ventral tegmental
1037 area revisited: is there an electrophysiological marker for dopaminergic
1038 neurons?. The Journal of physiology, 577(3), 907-924.
1039 Marsicano G, Lutz B (1999) Expression of the cannabinoid receptor CB1 in distinct
1040 neuronal subpopulations in the adult mouse forebrain. European Journal of
1041 Neuroscience 11:4213-4225.
1042 Martin-Santos, R., a Crippa, J., Batalla, A., Bhattacharyya, S., Atakan, Z., Borgwardt,
1043 S., ... & Zuardi, A. W. (2012). Acute effects of a single, oral dose of d9-
1044 tetrahydrocannabinol (THC) and cannabidiol (CBD) administration in healthy
1045 volunteers. Current pharmaceutical design, 18(32), 4966-4979.
1046 McPartland JM, Glass M, Pertwee RG (2007) Meta-analysis of cannabinoid ligand
1047 binding affinity and receptor distribution: interspecies differences. Br J Pharmacol
1048 152: 583–593.
1049 Meyer-Lindenberg AS, Olsen RK, Kohn PD, Brown T, Egan MF, Weinberger DR,
1050 Berman KF (2005) Regionally specific disturbance of dorsolateral prefrontal–
1051 hippocampal functional connectivity in schizophrenia. Archives of general
1052 psychiatry 62:379-386.
1053 Moreira FA, Guimarães FS (2005) Cannabidiol inhibits the hyperlocomotion induced by
1054 psychotomimetic drugs in mice. European journal of pharmacology 512:199-205.

1055 Morgan CA, Freeman TP, Powell J, Curran HV (2016) AKT1 genotype moderates the
1056 acute psychotomimetic effects of naturalistically smoked cannabis in young
1057 cannabis smokers. Transl Psychiatry, 6(2): 1–6
1058 Morrison PD, Nottage J, Stone JM, Bhattacharyya S, Tunstall N, Brenneisen R, Holt D,
1059 Wilson D, Sumich A, McGuire P (2011) Disruption of frontal theta coherence by Δ
1060 9-tetrahydrocannabinol is associated with positive psychotic symptoms.
1061 Neuropsychopharmacology 36:827.
1062 Norris C, Loureiro M, Kramar C, Zunder J, Renard J, Rushlow W, Laviolette SR (2016)
1063 Cannabidiol modulates fear memory formation through interactions with
1064 serotonergic transmission in the mesolimbic system. Neuropsychopharmacology
1065 41:2839.
1066 Nyiri G, Cserep C, Szabadits E, Mackie K, Freund T (2005) CB1 cannabinoid receptors
1067 are enriched in the perisynaptic annulus and on preterminal segments of
1068 hippocampal GABAergic axons. Neuroscience 136:811-822.
1069 Palaniyappan L, Simmonite M, White TP, Liddle EB, Liddle PF (2013) Neural primacy of
1070 the salience processing system in schizophrenia. Neuron 79:814-828.
1071 Park JB, Kwak H-J, Lee S-H (2008) Role of hyaluronan in glioma invasion. Cell
1072 adhesion & migration 2:202-207.
1073 Pertwee RG (2005) Inverse agonism and neutral antagonism at cannabinoid CB1
1074 receptors. Life sciences 76:1307-1324.
1075 Puighermanal E, Marsicano G, Busquets-Garcia A, Lutz B, Maldonado R, Ozaita A
1076 (2009) Cannabinoid modulation of hippocampal long-term memory is mediated
1077 by mTOR signaling. Nat Neurosci, 12(9): 1152-1158.

1078 Puighermanal E, Busquets-Garcia A, Gomis-González M, Marsicano G, Maldonado R,
1079 Ozaita A (2013) Dissociation of the pharmacological effects of THC by mTOR
1080 blockade. Neuropsychopharmacology, 38(7): 1334-1343.
1081 Ren, Y., Whittard, J., Higuera-Matas, A., Morris, C. V., & Hurd, Y. L. (2009).
1082 Cannabidiol, a nonpsychotropic component of cannabis, inhibits cue-induced
1083 heroin seeking and normalizes discrete mesolimbic neuronal disturbances.
1084 Journal of neuroscience, 29(47): 14764-14769.
1085 Renard J, Rosen LG, Loureiro M, De Oliveira C, Schmid S, Rushlow WJ, Laviolette SR
1086 (2017a) Adolescent cannabinoid exposure induces a persistent sub-cortical
1087 hyper-dopaminergic state and associated molecular adaptations in the prefrontal
1088 cortex. Cerebral Cortex 27:1297-1310.
1089 Renard J, Szkudlarek HJ, Kramar CP, Jobson CE, Moura K, Rushlow WJ, Laviolette SR
1090 (2017b) Adolescent THC exposure causes enduring prefrontal cortical disruption
1091 of GABAergic inhibition and dysregulation of sub-cortical dopamine function.
1092 Scientific reports 7:11420.
1093 Renard J, Loureiro M, Rosen LG, Zunder J, de Oliveira C, Schmid S, Rushlow WJ,
1094 Laviolette SR (2016) Cannabidiol counteracts amphetamine-induced neuronal
1095 and behavioral sensitization of the mesolimbic dopamine pathway through a
1096 novel mTOR/p70S6 kinase signaling pathway. Journal of Neuroscience 36:5160-
1097 5169.
1098 Rey AA, Purrio M, Viveros M-P, Lutz B (2012) Biphasic effects of cannabinoids in
1099 anxiety responses: CB1 and GABA B receptors in the balance of GABAergic and
1100 glutamatergic neurotransmission. Neuropsychopharmacology 37:2624.

1101 Ritov G, Ardi Z, Richter-Levin G (2014) Differential activation of amygdala, dorsal and
1102 ventral hippocampus following an exposure to a reminder of underwater trauma.
1103 Frontiers in behavioral neuroscience 8:18.
1104 Roberto M, Cruz M, Bajo M, Siggins GR, Parsons LH, Schweitzer P (2010) The
1105 endocannabinoid system tonically regulates inhibitory transmission and
1106 depresses the effect of ethanol in central amygdala. Neuropsychopharmacology
1107 35:1962.
1108 Russo, E. B. (2011). Taming THC: potential cannabis synergy and phytocannabinoid-
1109 terpenoid entourage effects. British journal of pharmacology, 163(7), 1344-1364.
1110 Salvati S, Natali F, Attorri L, Di Benedetto R, Leonardi F, Di Biase A, Ferri F, Fortuna S,
1111 Lorenzini P, Sanchez M (2008) Eicosapentaenoic acid stimulates the expression
1112 of myelin proteins in rat brain. Journal of neuroscience research 86:776-784.
1113 Schubart CD, Sommer IE, van Gastel WA, Goetgebuer RL, Kahn RS, Boks MP (2011)
1114 Cannabis with high cannabidiol content is associated with fewer psychotic
1115 experiences. Schizophrenia research 130:216-221.
1116 Selcher JC, Weeber EJ, Christian J, Nekrasova T, Landreth GE, Sweatt JD (2003) A
1117 role for ERK MAP kinase in physiologic temporal integration in hippocampal area
1118 CA1. Learning & memory 10:26-39.
1119 Solinas M, Massi P, Cinquina V, Valenti M, Bolognini D, Gariboldi M, Monti E, Rubino T,
1120 Parolaro D (2013) Cannabidiol, a non-psychoactive cannabinoid compound,
1121 inhibits proliferation and invasion in U87-MG and T98G glioma cells through a
1122 multitarget effect. PLoS One 8:e76918.

Szeszko PR, Goldberg E, Gunduz-Bruce H, Ashtari M, Robinson D, Malhotra AK, Lencz T, Bates J, Crandall DT, Kane JM (2003) Smaller anterior hippocampal formation volume in antipsychotic-naive patients with first-episode schizophrenia. American Journal of Psychiatry 160:2190-2197.

Takács VT, Szőnyi A, Freund TF, Nyiri G, Gulyás AI (2015) Quantitative ultrastructural analysis of basket and axo-axonic cell terminals in the mouse hippocampus. Brain Structure and Function 220:919-940.

Yuan P, Zhou R, Wang Y, Li X, Li J, Chen G, Guitart X, Manji HK (2010) Altered levels of extracellular signal-regulated kinase signaling proteins in postmortem frontal cortex of individuals with mood disorders and schizophrenia. Journal of affective disorders 124:164-169.

Zuardi AW, Hallak JE, Dursun SM, Morais SL, Sanches RF, Musty RE, Crippa JAS (2006) Cannabidiol monotherapy for treatment-resistant schizophrenia. Journal of Psychopharmacology 20:683-686.

Figure Legends

Figure 1. Acute effects of local (**a**) pERK1-2 expression, (**b**) ERK1-2 expression, and (**c**) pERK:ERK1-2 expression ratio in the vHipp of rats treated with VEH, THC (100 ng), CBD (100 ng), THC+CBD (100 ng+100 ng), THC+U0126 (100 ng+1μg), and THC+CBD+EPA (100 ng+100 ng+1 mM). (**d**) Representative western blot for pERK1-2 and ERK1-2 expression levels, relative to alpha (a)-tubulin in the vHipp. (**e**) Histological localization of microinfusion sites in the vHipp for each treatment condition (circles: Vehicle; diamonds: THC; stars: CBD; triangles: THC+CBD; squares: THC+U0126; and inverted triangles: THC+CBD+EPA). All drug doses were given in a total volume of 0.5 μl. n=5-6 rats, Mixed measures ANOVAs; *Indicates $p < 0.05$, **Indicates $p < 0.01$. Error bars represent the standard error of the means (SEM). pERK: phosphorylated Extracellular-signal Regulated Kinase; vHipp: ventral hippocampus; VEH: vehicle; THC: Δ-9-tetrahydrocannabinol; CBD: cannabidiol; EPA: eicosapentaenoic acid.

Figure 2. Effects of intra-vHipp VEH, THC (10 and 100 ng), CBD (10 and 100 ng), THC+CBD (100 ng+100 ng), THC+U0126 (100 ng+0.1 and 1μg), and THC+CBD+EPA (100 ng+100 ng+0.1 and 1 mM) on (**a**) distance travelled, and (**b**) time in centre compartment during the open-field test. (**c**) Representative activity plots for Vehicle, THC (100 ng), THC+CBD (100 ng+100 ng), and THC+CBD+EPA (100 ng+100 ng+1 mM) groups. (**d**) Depiction of light-dark anxiety test. Effects of intra-vHipp drug treatment on (**e**) % time spent in light side, and (**f**) latency to emerge from dark-light in the light-dark anxiety test. n=8-12 rats, one-way ANOVAs; *Indicates $p < 0.05$, **Indicates $p < 0.01$, ^Indicates $p < 0.05$ relative to all other groups. Error bars represent the standard error of the means

(SEM). vHipp: ventral hippocampus; VEH: vehicle; THC: Δ-9-tetrahydrocannabinol; CBD: cannabidiol; EPA: eicosapentaenoic acid.

Figure 3. Effects of intra-vHipp drug treatments on rewarding and aversive memory formation. (**a**) Photomicrograph demonstrating a representative vHipp microinfusion site. (**b**) Effects of intra-vHipp VEH, THC (10 and 100 ng), CBD (10 and 100 ng), THC+CBD (100 ng+100 ng), THC+U0126 (100 ng+1μg), and THC+CBD+EPA (100 ng+100 ng+1 mM) on % time freezing to contextual, and (**c**) olfactory-associative CS+ and CS- cues, (**d**) % time spent in morphine and saline-paired contexts during subreward threshold morphine (0.05 mg/kg, i.p.) CPP testing, (**e**) sucrose preference, and (**f**) water intake during sucrose preference testing. Intra-vHipp drug infusion occurred prior to each conditioning session. n=7-11 rats, one-way, or mixed measures ANOVAs; *Indicates $p < 0.05$, **Indicates $p < 0.01$. Error bars represent the standard error of the means (SEM). vHipp: ventral hippocampus; VEH: vehicle; THC: Δ-9-tetrahydrocannabinol; CBD: cannabidiol; EPA: eicosapentaenoic acid; CS: conditioned stimulus; CPP: conditioned place preference.

Figure 4. Effects of intra-vHipp VEH, THC (100 ng), CBD (100 ng), THC+CBD (100 ng+100 ng), and THC+U0126 (100 ng+1 μg) exposure on spontaneous VTA putative DA neuronal activity. (**a**) Microphotograph of a representative VTA microinfusion site. (**b**) VTA neuronal recording placement. (**c**) Summary of the VTA DA neuronal activity profile (ie, number of cells that increased, decreased, or did not change their firing frequency after microinfusions). (**d**) Consequences of intra-vHipp drug treatments on VTA DA neuronal firing frequency, and (**e**) burst rate. (**f**) Representative histogram showing the increase in response activity of one

DA neuron upon microinfusion of THC, and (**g**) example of a DA neuron showing no change in activity level following THC+CBD co-infusion. For each panel, inset shows (1) the action potential waveform of the selected neuron; and (2) show the activity patterns recorded before (baseline activity) and after the microinfusions respectively. n=12-16 cells from n=4-6 rats, one-way ANOVAs; *Indicates $p < 0.05$, **Indicates $p < 0.01$. Error bars represent the standard error of the means (SEM). vHipp: ventral hippocampus; VEH: vehicle; THC: ∆-9-tetrahydrocannabinol; CBD: cannabidiol; VTA: ventral tegmental area; DA: dopamine.

Figure 5. Effects of intra-vHipp VEH, THC (100 ng), CBD (100 ng), THC+CBD (100 ng+100 ng), and THC+U0126 (100 ng+1 μg) exposure on VTA non-DA (putative GABA interneurons) activity. (**a**) Summary of the VTA non-DA neuronal activity profile (ie, number of cells that increased, decreased, or did not change their firing frequency after microinfusions). (**b**) Consequences of intra-vHipp drug infusion on VTA GABA neuronal firing frequency. (**c**) Representative histogram showing the decrease in tonic firing frequency of a single VTA non-DA neuron upon microinfusion of THC, and (**d**) example of a non-DA neuron showing a non-significant increase in frequency levels following THC+CBD co-infusion. For each panel, inset shows (1) the action potential waveform of the selected neuron; and (2) show the activity patterns recorded before (baseline activity) and after the microinfusions respectively. n=11-15 cells from n=4-6 rats, one-way ANOVAs; *Indicates $p < 0.05$, **Indicates $p < 0.01$. Error bars represent the standard error of the means (SEM). vHipp: ventral hippocampus; VEH: vehicle; THC: ∆-9-tetrahydrocannabinol; CBD: cannabidiol; VTA: ventral tegmental area; DA: dopamine; GABA: Gamma-Aminobutyric Acid.

Figure 6. Effects of intra-vHipp VEH, THC (100 ng), CBD (100 ng), THC+CBD (100 ng+100 ng), and THC+U0126 (100 ng+1 μg) exposure on β (15-30 Hz), γ (30-80 Hz), and ε (90-100 Hz) oscillatory power in the VTA of a urethane anesthetized rat. (**a**) Representative spectrogram showing temporal changes in the power of intra-VTA oscillations at different frequencies. The power values are color-coded as indicated on the right-hand side insets. A peak at around 60 Hz reflect power line frequency and the LFP power values for frequencies between 59–61 Hz were excluded from further analysis. (**b**) Average normalized power spectra corresponding to LFP of VEH- (blue) and THC-treated (red) rats. Note the increased power of β (15-30 Hz), γ (30-80 Hz), and ε (90-100 Hz) bands in THC-treated rats. (**c-e**) Bar graphs summarizing the average total power change of the different frequency bands following intra-vHipp drug microinfusion. n=12-16 from n=4-6 rats, one-way ANOVAs; *Indicates $p < 0.05$, **Indicates $p < 0.01$. Error bars represent the standard error of the means (SEM). vHipp: ventral hippocampus; VEH: vehicle; THC: Δ-9-tetrahydrocannabinol; CBD: cannabidiol; β: beta; γ: gamma; ε: epsilon; LFP: local field potential; VTA: ventral tegmental area.

Figure 1

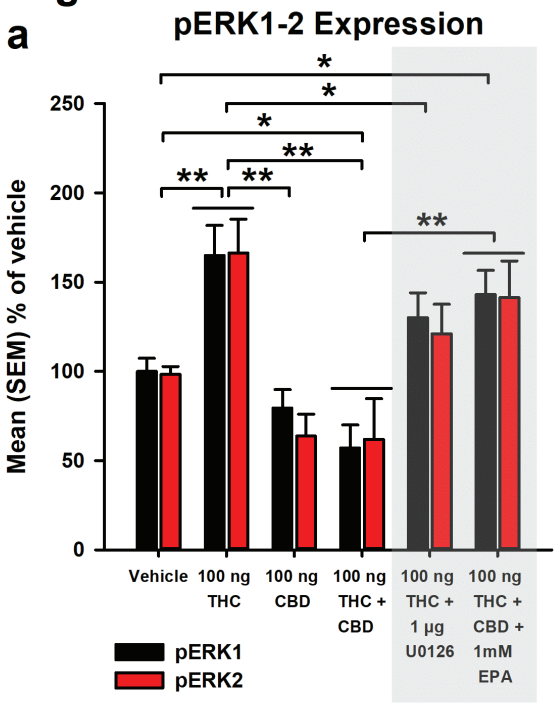

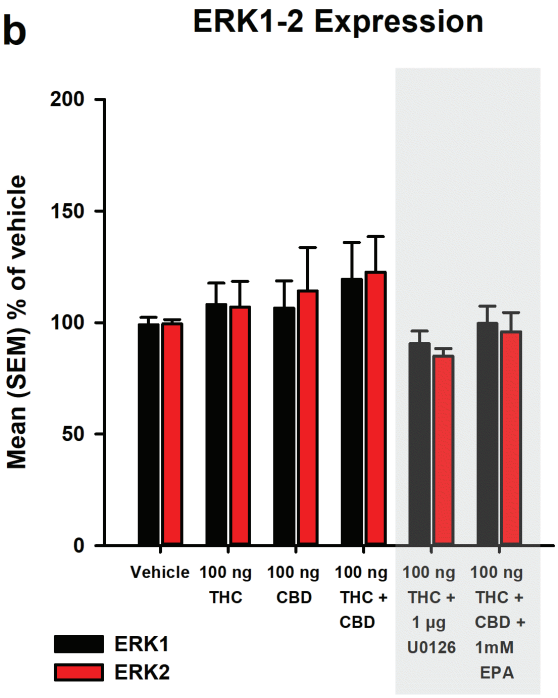

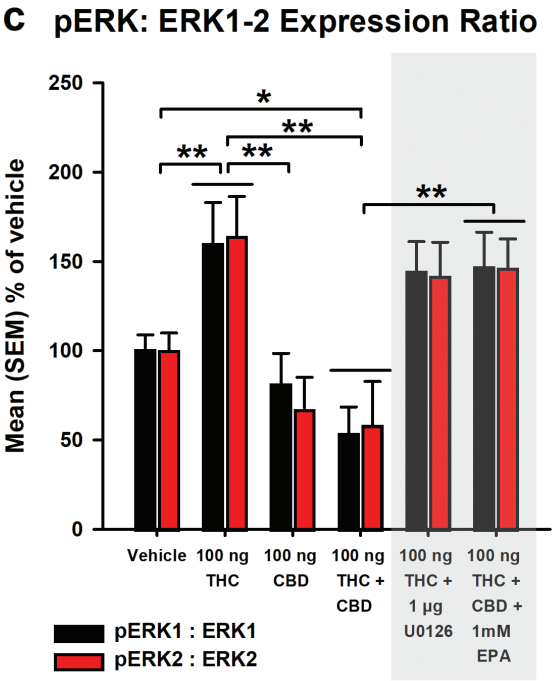

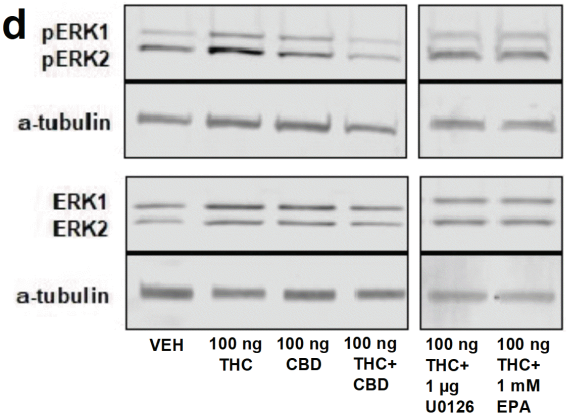

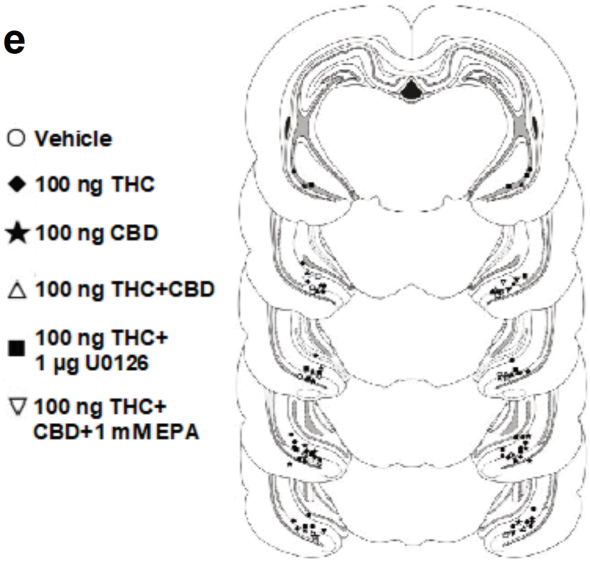

Figure 2

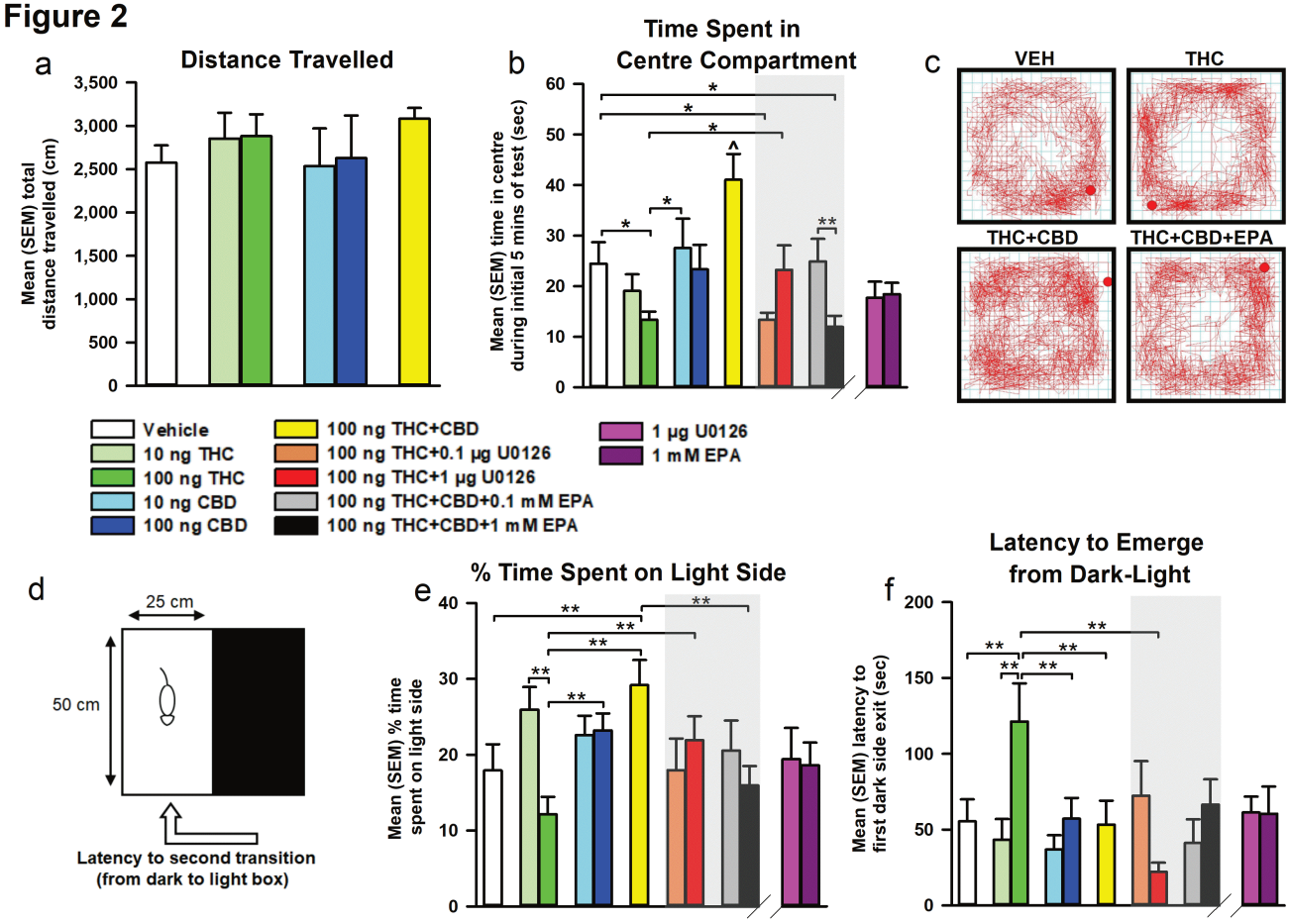

Figure 3

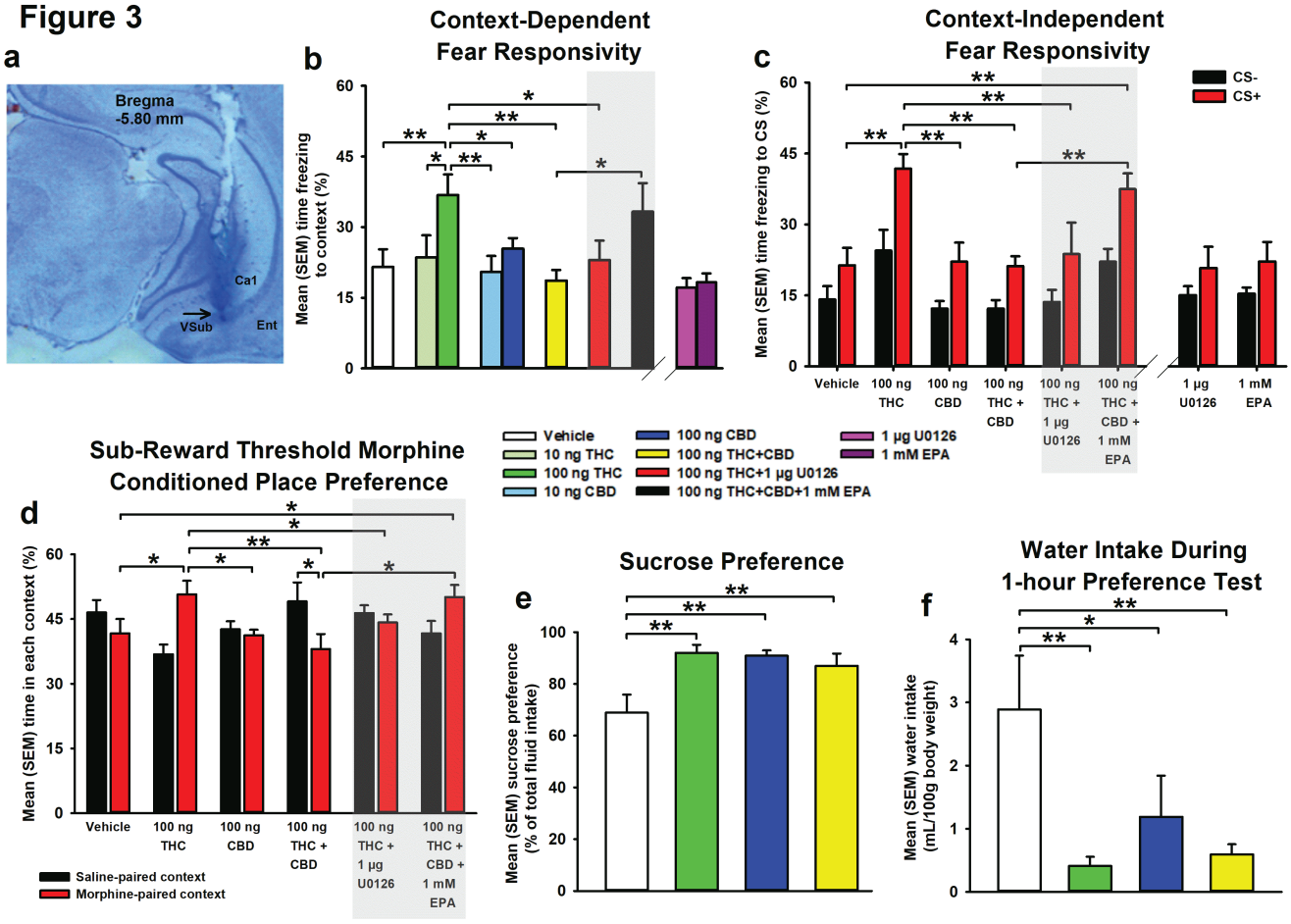

Figure 4

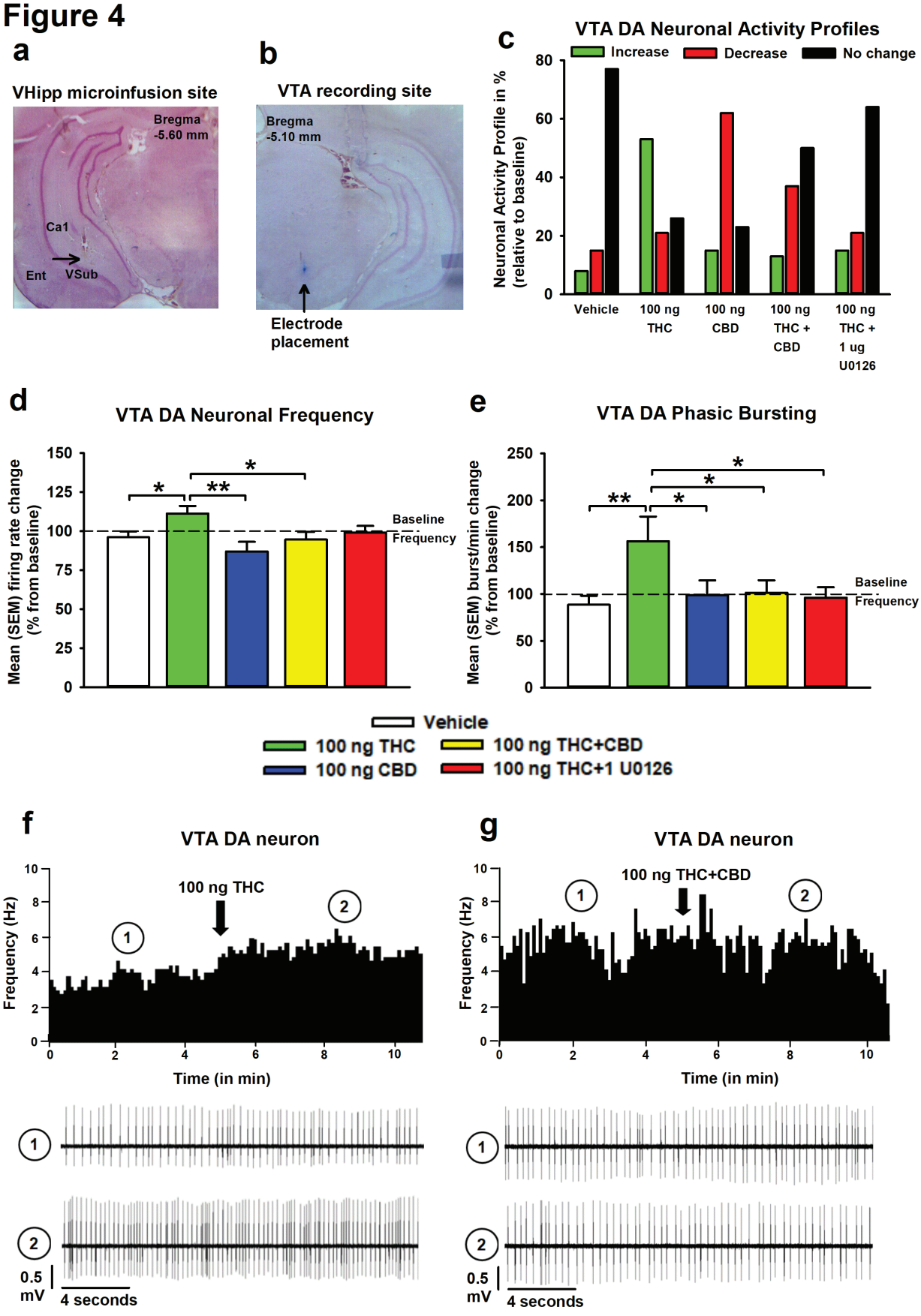

Figure 5

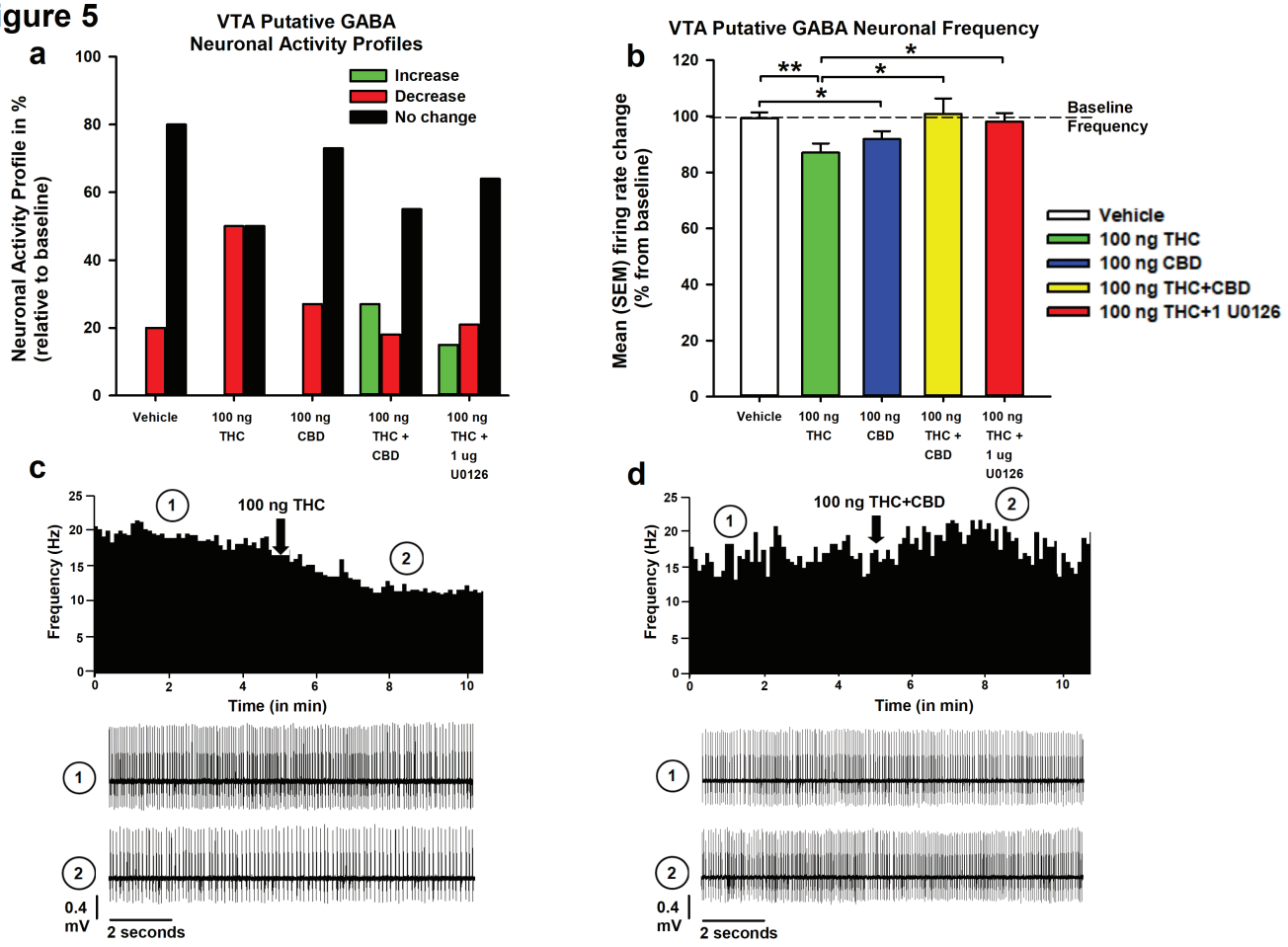

Figure 6